ORIGINAL ARTICLE

lajss.org Latin American Journal of Solids and Structures

www.lajss.org

Optimization of Profiled Steel Deck Composite Slab Strengthened with CFRP: A Finite Element Analysis Approach

Karthiga.S[a], **Umamaheswari.N**[b*]

[a]Department of Civil Engineering, SRM Institute of Science and Technology, Kattankulathur, Chengalpet, India – 603203.
Email: karthigs@srmist.edu.in
[b]Department of Civil Engineering, SRM Institute of Science and Technology, Kattankulathur, Chengalpet, India – 603203.
Email: umamahen@srmist.edu.in

* Corresponding author

https://doi.org/10.1590/1679-78258143

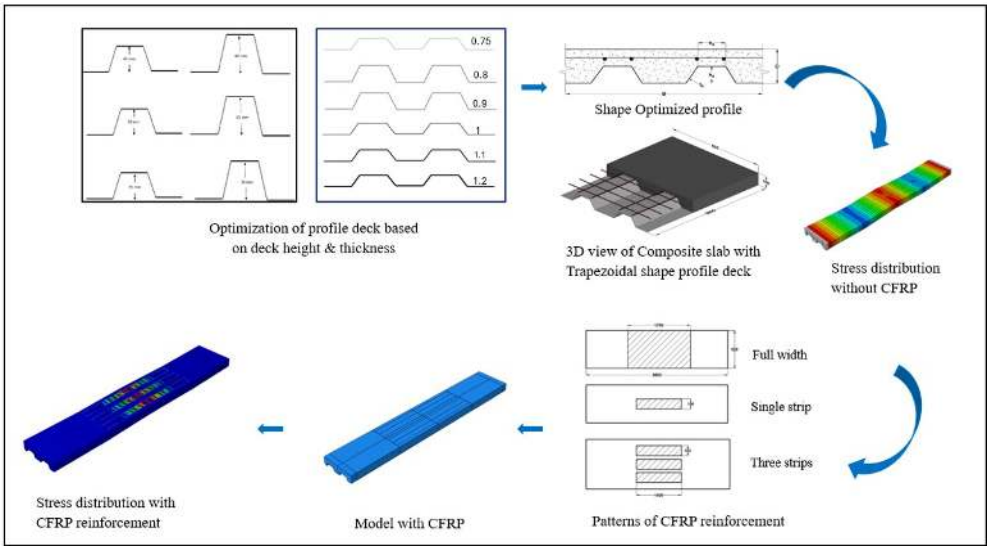
Abstract

This work leverages Finite Element (FE) modelling to optimise the deck geometry in continuous composite slab systems, focusing on trapezoidal profile decks. Subsequently, it examines the effectiveness of reinforcing the hogging moment area with Carbon Fiber Reinforced Polymer (CFRP). The main objective is to improve the structural performance when subjected to static loads by optimising geometric factors such as deck height and thickness. The deck profile that yielded the best results had a height of 60 mm, a thickness of 1 mm, and a shear span of 850 mm and resulted in a 7.6% increase in the ultimate load compared to a deck with a thickness of 0.75 mm. The study also assesses the impacts of CFRP reinforcement configurations. The optimal outcome was attained by utilising carbon fiber reinforced polymer (CFRP) sheets that spanned the whole width of the slab for a length of 1.7 m, resulted in a significant 43.17% enhancement in ultimate load. The CFRP enhanced slab, which spans the whole width, demonstrated a maximum load-carrying capability of 176.78 kN. Theoretical analysis indicated a high level of concurrence with FEM.

Keywords

Continuous Composite slab, CFRP, Trapezoidal steel decking, Finite Element Analysis, Negative moment region.

Graphical Abstract



Received: April 05, 2024. In revised form: May 16, 2024. Accepted: May 17, 2024. Available online: May 24, 2024
https://doi.org/10.1590/1679-78258143

Latin American Journal of Solids and Structures. ISSN 1679-7825. Copyright © 2024. This is an Open Access article distributed under the terms of the Creative Commons Attribution License, which permits unrestricted use, distribution, and reproduction in any medium, provided the original work is properly cited.

1 INTRODUCTION

The advent of composite construction has heralded significant advancements in the efficiency and performance of modern structural systems. Due to its inherent strength, durability, and ease of installation profiled steel deck composite slab systems have become a fundamental component in the field of construction (Abas et al., 2013; Gholamhoseini, 2018; Gholamhoseini et al., 2016, 2018; Hossain et al., 2019). By integrating the concrete's compressive strength with tensile strength of steel these systems lead to an optimized structural component that is both lightweight and robust. As seen in Figure 1 (a) and (b), profiled steel sheeting typically comes in two basic forms: re-entrant and trapezoidal. In a re-entrant profile, frictional interlock is used to provide composite action, whereas embossment or mechanical interlock is used in a trapezoidal deck sheet (John et al., 2022; Karimipanah et al., 2024). The composite action of steel decking and hardened concrete depends on the transfer of horizontal shear stresses at the interface between the slab and the steel decking (Johnson & Lee, 1977; Oehlers & Bradford, 1995; Stark, 1978). Enhancing composite motion between components may be achieved effectively by using embossment (Karimipanah et al., 2024). According to several researches (de Andrade et al., 2004; Faust, 1997; Ferrer et al., 2006; Marimuthu et al., 2007; Mohammed et al., 2011), embossment in the profiled sheets increased the composite action of the slabs by preventing slippage between the concrete and the profiled sheets. In further studies, the variations in steel sheets thicknesses and the sizes, forms, and positions of embossments were examined (Crisinel & Marimon, 2004; Makelainen & Sun, 1998; Mohan Ganesh et al., 2005; Vainiūnas et al., 2006). Nevertheless, despite their extensive implementation, there persists an ongoing pursuit for enhancement, specifically about the optimisation of the geometric configuration of the steel deck and the augmentation of its structural robustness by inventive reinforcing methodologies

In most cases, the steel decking is delivered in lengths that are two spans long, and during the construction process, negative reinforcement is placed at the top of the slabs above the mid-support. Because of this, the composite slab is generally continuous (Gholamhoseini, 2018). As the corrugated profiles of the decks used are only in one direction the load impact is transferred along the ribs' direction (Hofmeyer et al., 2002; Wright et al., 1987). Regardless, real engineers often benefit from using linear-elastic analysis and assuming the slab is simply supported in ultimate limit states. Incorporating mesh reinforcement into composite concrete slabs results in higher construction costs and complexity, as well as slower erection. Therefore, it is more cost-effective to replace conventional reinforcing, such as rebar or mesh, partially or completely with alternative types of crack control. Steel fibre reinforced concrete (SFRC) is a promising solution that can enhance structural performance (Abas et al., 2013; Gholamhoseini et al., 2016). The implementation of this technology has several advantages, such as enhanced load-bearing capacity of slabs, enhanced fracture management, controlled interface slide under plastic loading, and heightened fire resistance. These advantages can lead to cost savings (Abas et al., 2013; Congro et al., 2021; Gholamhoseini et al., 2016; Lin et al., 2014; Rahimi Mansour et al., 2015). Aside from steel fibres, fibre reinforced polymer (FRP) is used in concrete through external bond (EB) is an alternate method to enhance the moment capacity and control crack. For decades, reinforced concrete beams and slabs have been strengthened with externally bonded (EB) fibre reinforced polymer laminates. Research has shown that FRP may effectively slow the spread of cracks and enhance the flexural performance of reinforced concrete elements (Anil et al., 2013; Li-Xiang et al., 2021; Smith et al., 2011; Zhang et al., 2021). Numerous researchers have investigated the use of FRP in reinforcing reinforced concrete and composite beams via external bonding for decades. Their findings indicate that FRP effectively retards fracture propagation and tends to improve the flexural performance of members (Anil et al., 2013; Li-Xiang et al., 2021; Smith et al., 2011). The increased inclination towards the utilisation of Carbon Fibre Reinforced Polymer (CFRP) in reinforcing applications may be ascribed to its remarkable strength-to-weight ratio and the long-lasting nature of CFRP materials. This characteristic renders it a more advantageous alternative in comparison to traditional techniques of reinforcement (Bank & Arora, 2007; Houssam et al., 2012; Li et al., 2019; Razaqpur et al., 2020; Wang et al., 2018). Many studies have demonstrated that one-way reinforced concrete (RC) slabs reinforced with carbon fiber reinforced polymer (CFRP) have better fracture width management and higher load bearing capability (Zhou et al., 2023). In research done by Dalfré (Dalfré & Barros, 2013) about the performance of continuous reinforced concrete (RC) slabs reinforced with carbon fibre reinforced polymer (CFRP) using near-surface mounting, it was seen that the slabs' load capacity saw a notable improvement. However, it was also reported that there was a decrease in the redistribution of bending moments. The study conducted by Liu (Liu et al., 2022) investigated the influence of carbon fibre reinforced polymer (CFRP) on the negative bending moment regions of continuous composite beams. The investigation involved manipulating the number of CFRP layers and introducing a novel bonding technique. An analytical investigation of the flexural strength of composite columns reinforced with prestressed CFRP plates was performed by Jun Deng (Deng et al., 2011). In addition, Ayman El-Zohairy (El-Zohairy et al., 2017) conducted both experimental and analytical studies which showed that adding different layers of CFRP laminates to the negative bending moment areas of continuous composite beams led to a 22% enhancement in load capacity.

The use of numerical simulation has emerged as an important methodology within the realm of structural engineering research, particularly in addressing the complexities associated with intricate systems, costly testing methodologies, and limited experimental data. Ensuring the dependability of simulation outputs necessitates the meticulous selection of the material constitutive model for the composite slab and the correct input of model parameters. Finite element modelling was employed by many researchers to analyse composite slabs containing standard concrete. Ríos et al., 2017 used finite element (FE) modelling to investigate the shear-bond behaviour of composite slabs bending under various loading configurations. Floride and Cashell (Florides & Cashell, 2017) conducted numerical simulations of composite floor slabs experiencing significant deflections to replicate their behaviour when exposed to fire loads. Daniels and Crisinel, 1993 developed a finite element (FE) model employing plane beam components to evaluate the performance of composite slabs with a single or continuous span. They also conducted pullout tests to explain the shear interaction between concrete and steel. Veljkovic (Veljkovic, 1996) employed three-dimensional finite element (FE) analysis to examine the interface between the concrete and steel sheets in the composite slab. Abdullah and Easterling (Abdullah & Samuel Easterling, 2009) employed shear-bond slip curves inside FE models to forecast the horizontal shear bond characteristics in composite slabs. It was achieved by using radial-thrust connection elements between the concrete and steel deck. The bending test response of the composite slab was simulated in the finite element model developed by Widjaja (Widjaja, 1997), utilising two parallel Euler-Bernoulli beam components. The key issue in the finite element (FE) method was the interface contact between the specified profiled sheet and concrete. In their study, Ferrer et al.(Ferrer et al., 2006) used finite element (FE) methodology to simulate composite slab to perform pullout tests. They considered various friction coefficients for the steel-concrete interface contact components.



Figure 1 Shape of profile deck (a) Trapezoidal deck (b) Re-entrant profile

Regarding all the above research works, the FE model was developed for the present study and the hogging moment region of the composite slab was strengthened by using CFRP adopting an external bonding technique. An investigation into the behaviour of continuous composite slabs was the primary subject of this work. The effect of parameters like deck height, deck thickness and shear span on the performance continuous composite is studied. After optimization of the profile deck, the CFRP strengthening on the hogging region of the slab is studied. The length, width, and number of layers of CFRP was taken as parameters. The study used FE models developed using ABAQUS. In the present study all the specimens were provided with the minimum code recommended reinforcement (EN, 1994) over the internal support of the continuous slab in addition to which the slabs were externally strengthened by carbon fiber reinforced polymer.

2 FINITE ELEMENT ANALYSIS

To achieve the stated objective of the study, a comprehensive analysis was conducted on a three-dimensional model using the commercial programme ABAQUS/CAE version 6.14 (Hibbitt & Sorensen, 2019). The present investigation involved the development of finite element models utilising "displacement control analysis" to effectively replicate the non-linear characteristics of the profile deck and CFRP strengthening. The parametric investigation utilises the various models developed in ABAQUS to study the behaviour of the specimen. The subsequent section provides an explanation of the modelling of different aspects within the model and material model.

2.1 Geometrical Modelling

In an analytical model, the composite slab is assembled from four parts: steel deck, concrete topping, shrinkage reinforcement, and shear stud. The Figures 2 (a) to 2 (d) depict the various slab components. The concrete component of the composite deck is simulated using the solid element C3D8R, a linear eight-node brick element with decreased integration that is suited for bending concerns and possible stiffness considerations. The profile steel deck is modelled using the S4R four-node quadrilateral shell element. The top reinforcement, which is mainly for shrinkage and temperature impact, is simulated as a beam

element embedded in the solid element of concrete to imitate perfect bonding in the concrete element. It is important to highlight that the reinforcements against temperature and shrinkage have no impact on the structural performance of composite slabs and are negligible. Additive to the components of the composite slab, the reinforcement achieved by CFRP was represented by a linear element B31. The axisymmetric revolution was employed to simulate the reinforcement at the top. The objective of this work was to develop a finite element (FE) method based on displacement. To enhance computational efficiency, a limited integration technique was employed. The results demonstrated that this approach yielded superior modelling of the composite slab behaviour compared to full integration. The analytical model simulates the experimental setup of the four-point bending and support conditions by assigning appropriate boundary conditions and subjecting it to a transverse displacement for the purpose of displacement control simulation. The displacements of all three degrees of freedom (DOF) were limited, with the vertical DOF displacements being assigned a value of -70 mm for the finite element (FE) models to simulate flexural loads. To represent the supports, the displacements in all three degrees of freedom (DOFs) were limited at the bottom two side ends of the slabs in a vertical manner. The displacement for all three degrees of freedom (DOFs) was released in the X and Z axes.

2.2 Material modelling

2.2.1 Concrete

Three approaches are available to represent the damage attributes of concrete in ABAQUS (Hibbitt & Sorensen, 2001) Furthermore, because the CDP was created based on crushing and cracking under tension and compression, respectively, it can forecast how concrete would behave in both situations as well as the features of damage. 1. Smeared crack model 2. Model of brittle cracks 3. The plasticity of concrete damage (CDP).

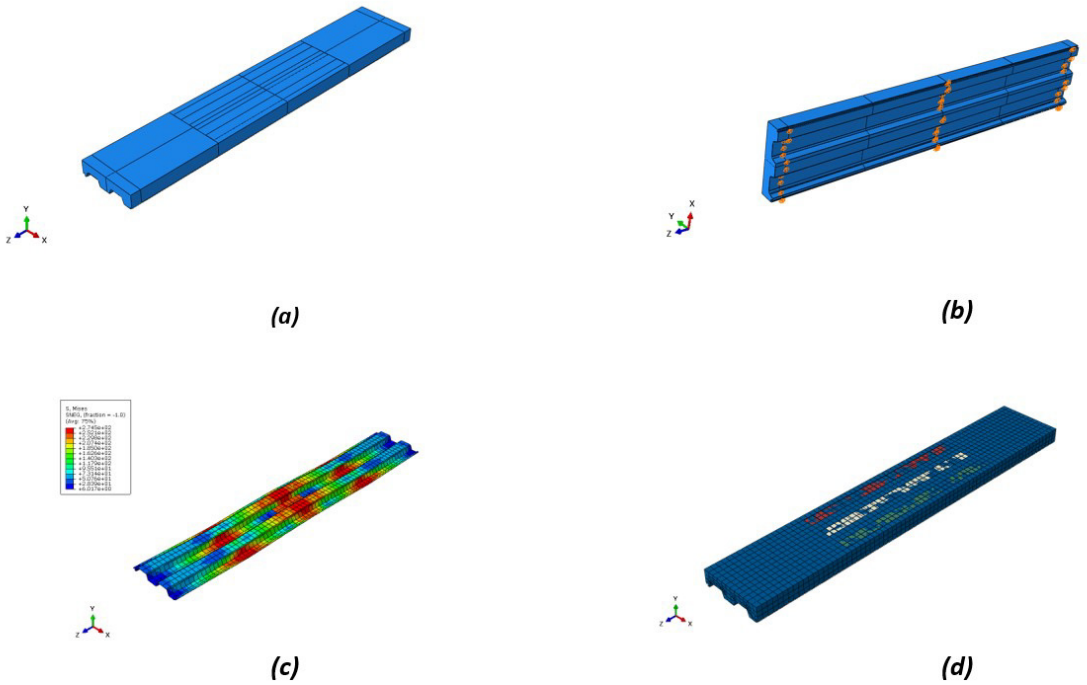


Figure 2 Finite Element model of continuous composite slab (a) Assembled model (b) Support condition (c) Meshing (d) Stress variation in profiled deck

For concrete models exposed to both static and dynamic load combinations, the concrete damage plasticity model is the recommended choice among the three models (Hibbitt & Sorensen, 2001). Furthermore, the CDP is capable of predicting the behaviour of concrete in both tension and compression, as well as damage characteristics, because it was designed based on crushing and cracking in tension and compression, respectively (Hibbitt & Sorensen, 2001)(Jeeho & Gregory L., 1998). The Figure 3 illustrates the compressive stress-strain behaviour of concrete. The current investigation's model described the concrete's inelastic properties by combining isotropic damaged elasticity with isotropic compressive and tensile plasticity. When pressure is applied uniaxially, the majority of concrete exhibits linear elastic behaviour until the failure stress (f't), which occurs after a softening branch as in Figure 4 [46]. The parameters d_t and d_c in ABAQUS represent the degradation of stiffness in compression and tension behaviour, respectively. They range from zero, indicating the undamaged state, to one, indicating complete loss of strength in the material. The above parameters for the model is defined for M30 grade of concrete. The tensile

properties of CFRP and compressive properties of concrete used in the study are shown in Table 1 and Table 2 (Diab et al., 2020). The model takes damage and plasticity effects into account in addition to the compressive and tensile behaviour of concrete. The damage and plasticity parameters are as mentioned below,

- Dilation Angle(ψ) -35°
- Flow potential Eccentricity (ε) - 0.1
- Ratio of Initial Biaxial Compressive Yield Stress to Initial Uniaxial Compressive Yield Stress (f_{bo}/f_{co})- 1.16
- Ratio of the Second Stress Invariant on the Tensile Meridian to that on the Compressive Meridian, (K)- 0.667
- Viscosity Parameter (μ)-0.007985
- Compressive yield stress – 30 N/mm^2
- Compressive plastic strain – 0.00359
- Tensile yield stress – 4.2 N/mm^2
- Tensile plastic strain - 0.0021

Table 1 CFRP and Epoxy Resin- Physical Properties

Material	Thickness, mm	Tensile strength, MPa	Ultimate strain	Modulus of Elasticity, E GPa
CFRP- unidirectional	0.13	3450	14,460	200
Epoxy	-	-	-	3.5

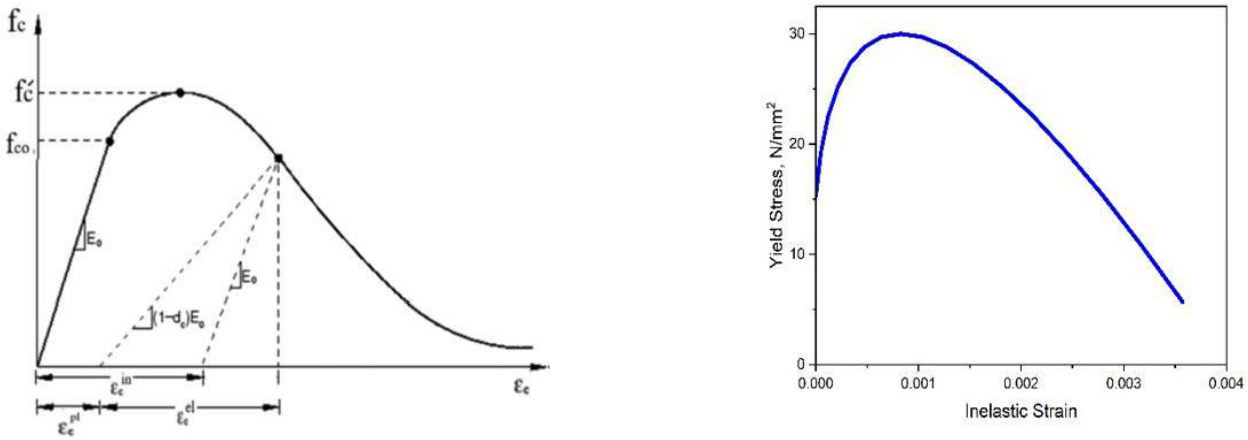


Figure 3 *Compression stress-strain response of concrete* (Hibbitt & Sorensen, 2019)

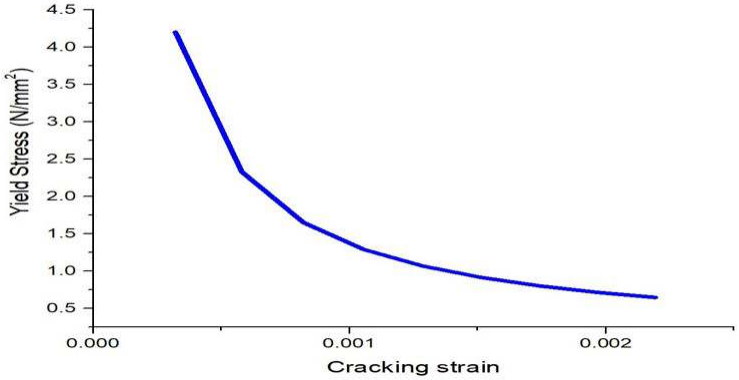


Figure 4 *Tensile stress-strain response of concrete* (Hibbitt & Sorensen, 2019)

2.2.2 Steel

The properties of the profile deck (stainless steel) used in the present study are as shown in Table 2 obtained from previous literature (Marimuthu et al., 2007). The profile deck shape, dimensions and three-dimensional view of the profile deck used in the study is as shown in Figure 5 and Figure 6. The values of true stress and logarithmic plastic strain can be derived by conducting a tensile coupon test on the samples cut from the profile deck steel. The same was calculated using the below Equations (1) and (2) by (Lubliner, 2008) to define the steel properties in ABAQUS for the current study.

$$\sigma_{true} = \sigma_{nom}\,(1 + \varepsilon_{nom}) \tag{1}$$

$$\varepsilon_{pl}^{ln} = \ln\,(1+ \varepsilon_{nom}) - \frac{\sigma_{true}}{E_S}\,) \tag{2}$$

Where, σ_{true} is the true stress, ε_{pl}^{ln} is logarithmic plastic strain, σ_{nom} represents the nominal stress, ε_{nom} is the nominal strain and E_s represents the modulus of elasticity of steel. The uniaxial tensile response of the profile sheet and reinforcing bars was simulated using the same approach. The behaviour of the material exhibited linearity until reaching the yield stress, at which point it transitioned into an inelastic state as it underwent hardening till reaching the ultimate stress.

Table 2 Properties of Profile steel deck and Concrete (Diab et al., 2020)

Material	Compressive strength, MPa	Tensile strength, MPa	Ultimate strain	Modulus of Elasticity, E GPa
Profile steel Deck	-	310	14,460	230
Concrete	36	-	0.0035	30

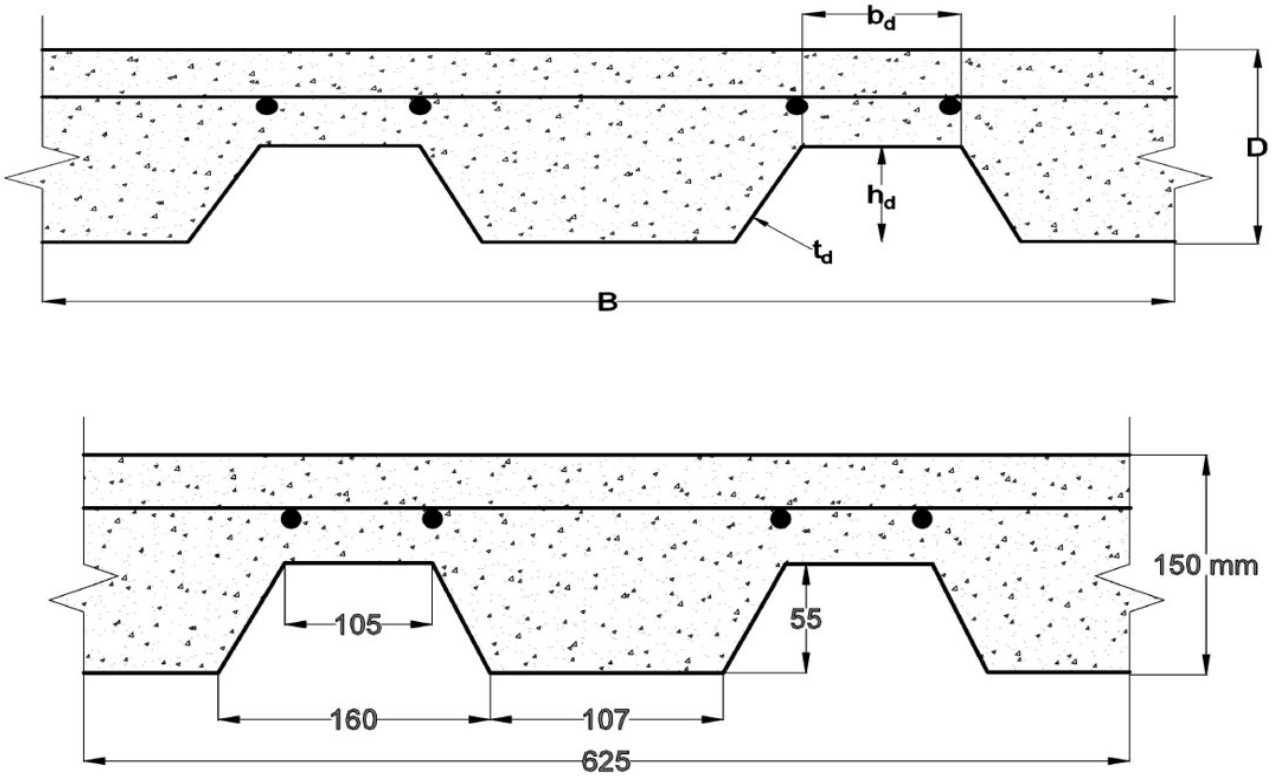


Figure 5 *Profile deck shape and dimensions* (Marimuthu et al., 2007)

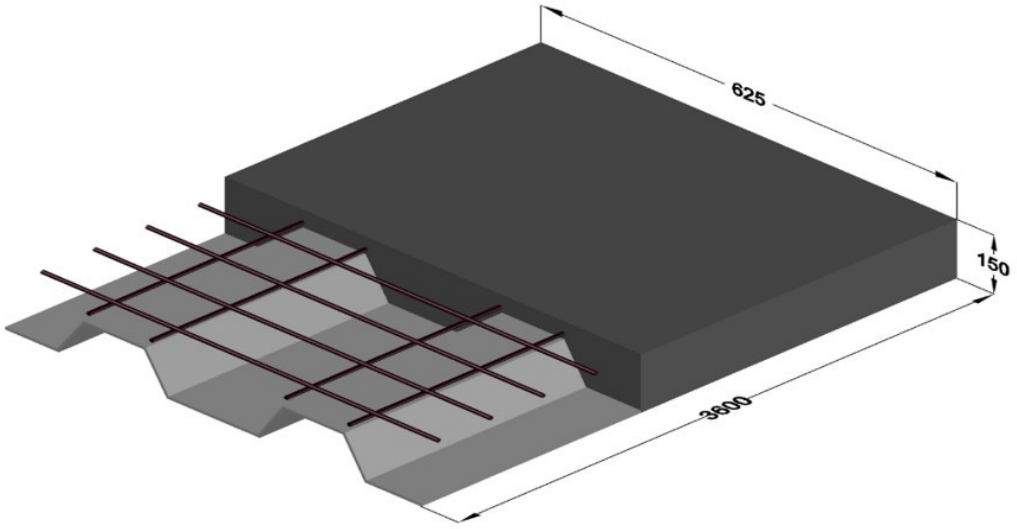


Figure 6 Profile deck in three-dimensional view

2.2.3 CFRP

A unidirectional CFRP fabric was used in the study and the properties of the carbon fibre used in the study is shown in Table 1. The different pattern of CFRP strips used for the present study is shown in Figure 7.

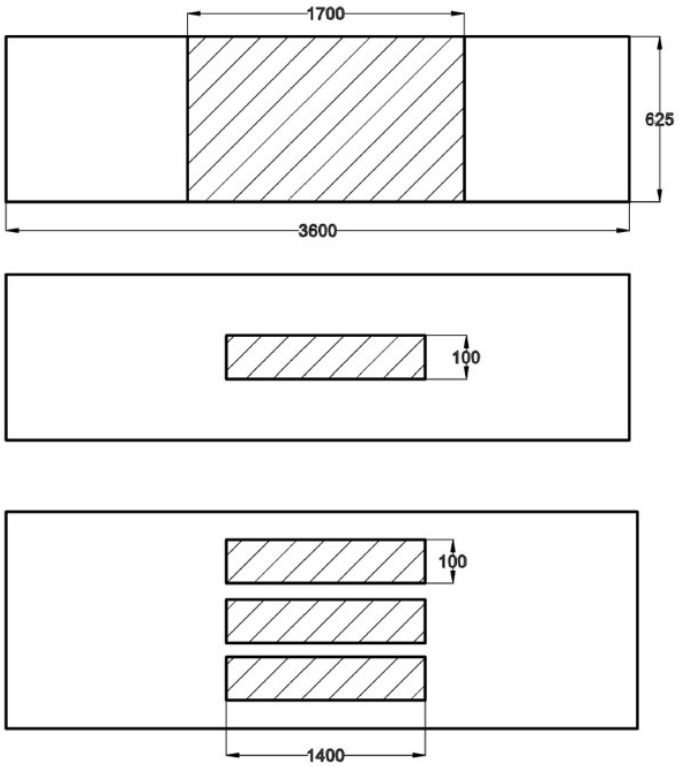


Figure 7 Patterns of CFRP reinforcement (a) Full width (b) Single strip at centre (c) Three strips at equal distance along width

2.3 Contact modelling, Boundary condition and Load

The model incorporates many types of interactions, including embedded region, tie constraint, and surface-to-surface contact as shown in Figure 8. The reinforcement bars are embedded in the concrete region. There exists a surface-to-surface interaction characterized by relatively small slippage between the steel deck and the concrete surface. The model exhibited tangential behaviour with a friction coefficient of 0.3 and resulted in strong contact. The CFRP and concrete are interconnected by a tie constraint. Adhesive is employed to connect two layers of CFRP when many layers are utilised. Nevertheless, the

delamination failure occurred due to the adhesive layers being subjected to both tension and shear loads simultaneously. In this work, the cohesive laws are applied to the adhesive layer, which is positioned underneath a mixed-mode zone known as mixed-mode delamination. There are two types of delamination that can occur on a cohesive surface (Kazem et al., 2018) mode I, which is produced by pure tension, and mode II, which is generated by pure shear. By employing finite element modelling and utilising mixed mode delamination for the adhesive material, the researchers were able to obtain accurate outcomes that closely aligned with their experimental investigations (Abdulrazzaq et al., 2022)(Cifuentes & Medina, 2013) . The boundary conditions used in the present study to model a continuous composite slab is pinned and roller support conditions. The end supports are given as side rollers with $u_1=u_2=0$ $u_3 \neq 0$ and the central support is provided as pinned with $u_1=u_2=u_3=0$. Two-point load is given based on shear span using displacement-based approach.

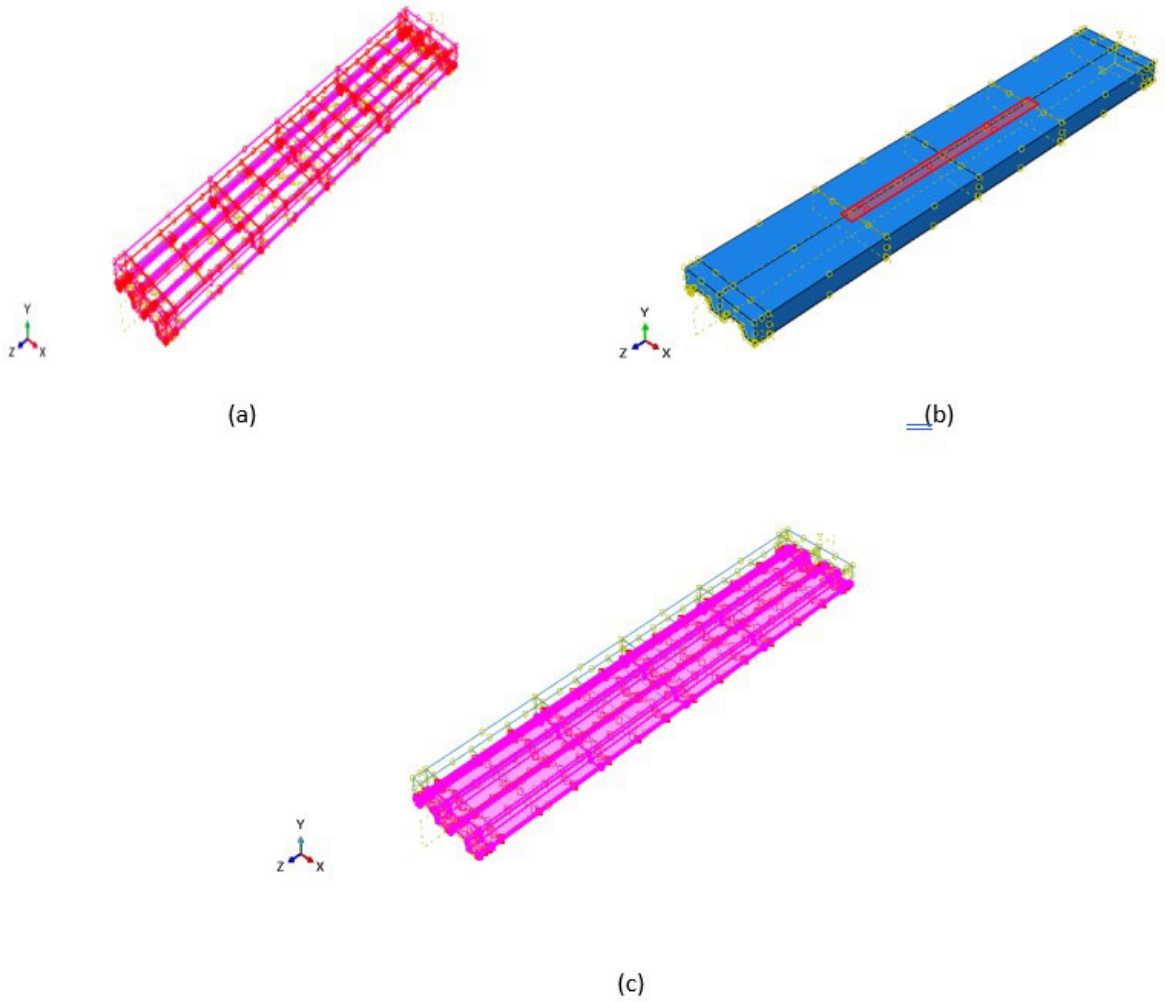


Figure 8 Contact modelling used in the model (a) Surface to surface interaction (b) Tie Constraint (c) Embedded region

2.4 Meshing

The mesh size utilised in the study significantly influences the correct depiction of outcomes. There is a positive correlation between the finer mesh size and the ability to bear load and displacement at mid span. As the mesh size increased, the accuracy of FEM further decreased. Overall, the utilisation of a revised mesh led to studies that exhibited higher accuracy, but at the expense of increased computing costs. Therefore, the optimal approach was to select a mesh size that yielded satisfactory outcomes. A hexahedral element with sweep technique was used to mesh the assembly of all components in the model. The finite element model of the composite slab was developed for the present study, employing a global seed size of 50 mm for each individual component. A total of 25409 elements were utilised to construct the finite element composite slab model. Among them, 23422 elements were utilised for concrete (C3D8R), 1687 elements were used for steel linear quadrilaterals of type S4R, and 300 elements were used for CFRP linear line elements in model C5. The remaining models were similarly meshed using a comparable approach. The components of the model with their respective mesh are shown in Figure 9.

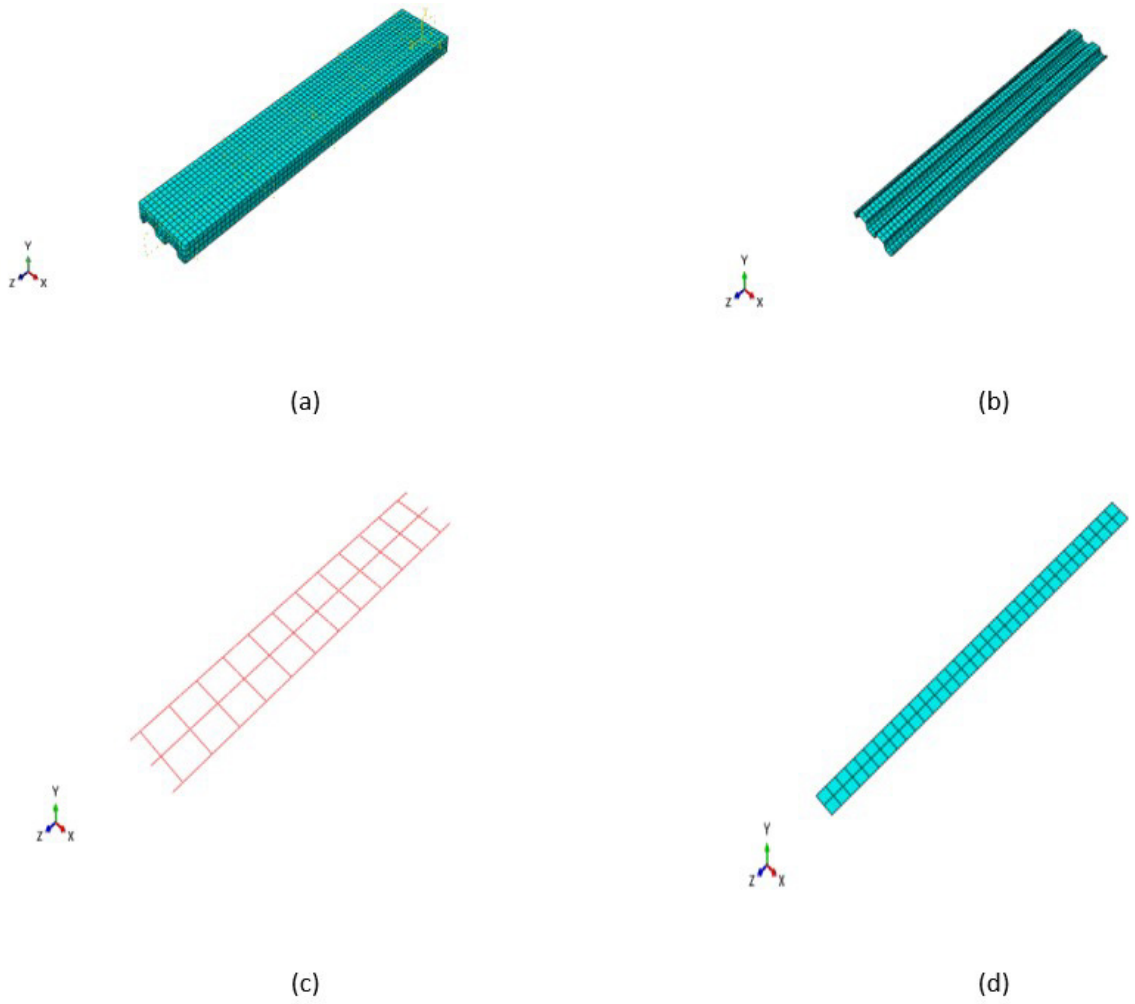


Figure 9 Meshing of the model components (a) Concrete portion (b) Profile deck (c) Rebar (d) CFRP.

2.5 Validation

To evaluate the accuracy of the finite element model used in the present study, the model was validated with two previous experimental work performed by Saravanan et al. (Saravanan et al., 2012) and Abas et al. (Abas et al., 2013). The validation of the model was done using two different study. The work conducted (Saravanan et al., 2012) focused on a composite slab system including a cold form deck with a trapezoidal shape, which was subjected to static stress. A total of 6 specimens of size 3100 mm × 900 mm were studied under static and cyclic load for different shear spans. The model is verified using a specimen with a short shear span of 350 mm under static load. The findings are displayed in Figure 10 (a). The model accurately predicted the findings from the load displacement graphs, with a slight deviation of 4% compared to the actual study. A comprehensive investigation was conducted by Abas et al on continuous composite slabs, whereby they tested a total of eight two-span continuous composite slabs. Every specimen is positioned on a profile deck with dimensions of 7000 mm in length and 700 mm in breadth. The load versus displacement characteristics of the two-span continuous slab with each span of 3400 mm are employed to validate the finite element (FE) model, as seen in Figure 10 (b). The model's predictions exhibited a high level of concurrence with the experimental findings, with a margin of error of 4%. Table 3 presents the load and displacement values obtained from the finite element (FE) model and experimental studies employed for validation purposes.

Table 3 Comparison of ultimate Load and Displacement values of predicted model and previous experiments

Description	Load, kN	Displacement, mm	Percentage error
FE model	55.76	64	+4.03%
Saravanan et al.(Saravanan et al., 2012)	54.00	64	-
FE model	67.19	53	+4.04%
Abas et al.(Abas et al., 2013)	70.00	51	-

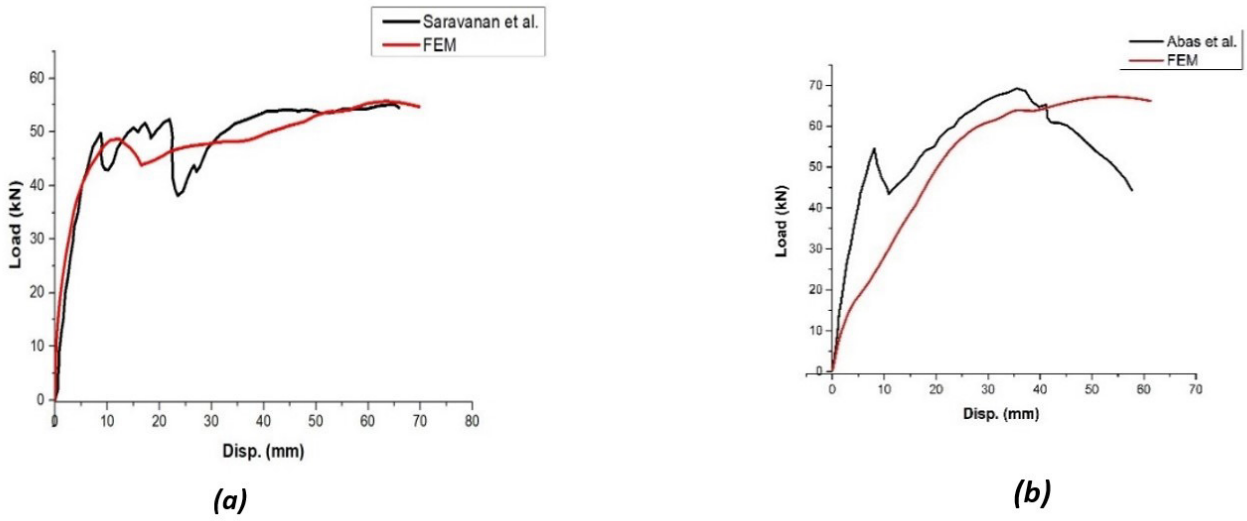


Figure 10 *Load vs Displacement of predicted and experimental work (a) Saravanan et al.*(Saravanan et al., 2012) *b) Abas et al.*(Abas et al., 2013)

3. PARAMETRIC ANALYSIS

The parametric analysis aims to optimize the profiled deck sheet by the influencing parameters such as deck height and thickness. The shear span is also considered to study the overall effect of the continuous composite slab under flexure. The effective length of continuous slab is 3400 mm. The shear span is considered as L/4, L/6, and L/8. Initial consideration of deck height, thickness, and shear span of 45, 0.75 and 850 mm respectively. The deck height is varied between 45 mm to 70 mm with incrementation of 5 mm each. Similarly, the deck thickness is varied as 0.75, 0.8 ,0.9,1,1.1 and 1.2 mm. From the optimized set of profiled deck configuration, the slab is externally strengthened in the hogging region of continuous slab using CFRP wrapping. The external bond technique helps to improve the negative moment capacity and limit the crack width over the internal support of the slab. The CFRP strengthening is also critically analysed based on the positioning of CFRP by varying the length (1.4 m and 1.7 m), Width (strip and full width) and number of layers (single and two layers). A total of 24 models were analysed as shown in Table 4 and 5 and the results of the same are given in Table 6.

Table 4 Parameters considered for analysis of continuous composite slab

Model ID	Parameters Analyzed						
	Height of deck (mm)	Thickness of the deck (mm)	Shear span (mm)	CFRP Parameters			
				Length of CFRP	Width of CFRP	Layers of CFRP	Description
M1	45	0.75	850	-	-	-	Effect of Deck height was studied
M2	50			-	-	-	
M3	55			-	-	-	
M4	60			-	-	-	
M5	65			-	-	-	
M6	70			-	-	-	
M7	60	0.75	560	-	-	-	Effect of Shear Span was studied
M8	60		425	-	-	-	
M9	60	0.80	850	-	-	-	Effect of thickness of deck was studied
M10	60	0.90		-	-	-	
M11	60	1.00		-	-	-	
M12	60	1.10		-	-	-	
M13	60	1.20		-	-	-	

Table 5 Parameters considered for analysis of continuous composite slab reinforced with CFRP

Model ID	Parameters Analyzed						
	Height of deck (mm)	Thickness of the deck (mm)	Shear span (mm)	CFRP Parameters			
				Length of CFRP	Width of CFRP	Layers of CFRP	Description
CF1	60	1	850	1.7	Full	1	*Compared for effect of length
CF2				1.4	Full	1	CF1 and CF2
CF3				1.7	3 strips	1	CF3 and CF4
CF4				1.4	3 strips	1	CF6 and CF8 CF7 and CF9
CF5				1.7+1.4	1 strip	2	*Compared for effect of layers
CF6				1.7	1 strip	1	CF6 and CF7 CF8 and CF9
CF7				1.7	1 strip	2	*Compared for effect of width
CF8				1.4	1 strip	1	CF1, CF3 and CF6 CF2, CF4 and CF8
CF9				1.4	1 strip	2	
CF10				1.7+1.4	3 strips	2	CF5, CF10 and CF11
CF11				1.7+1.4	Full	2	

Table 6 Results of parametric analysis of composite continuous slab

Specimen	Ultimate peak load, kN	Mid span Deflection at peak load, mm	Energy based ductility J	End slip, mm
M1	105.34	15.73	1386	7.41
M2	107.17	17.25	2285	5.98
M3	106.28	17.68	2223	6.13
M4	108.38	19.02	2284	7.41
M5	104.88	17.55	2200	5.98
M6	103.11	18.05	2164	6.13
M7	96.32	19.83	2090	5.8
M8	105.32	17.35	2160	5.75
M9	108.76	17.79	2290	5.59
M10	112.77	17.51	2365	7.00
M11	116.67	17.21	2429	7.67
M12	120.33	16.67	2529	5.93
M13	123.89	16.75	2602	6.03
CF1	167.04	20.04	2063	4.90
CF2	137.94	43.30	2375	7.45
CF3	141.85	19.74	1005	1.92
CF4	104.08	36.98	1471	7.14
CF5	117.51	18.91	1517	5.21
CF6	109.88	18.43	1536	5.4
CF7	117.62	18.93	1512	5.18
CF8	80.13	15.61	1316	7.89
CF9	86.06	14.97	485	3.25
CF10	140.07	14.28	1288	1.27
CF11	176.78	20.88	1681	4.50

3.1 Optimization of profile deck

The profiled deck has been meticulously optimized to enhance the structural efficiency and performance, leveraging its geometric parameters. Finite element (FE) analysis has been employed to scrutinize the impact of deck height, thickness, and shear span. Table 6 delineates the findings, with Models M1 to M6 elucidating the influence of deck height, Models M7 to M10 examining shear span effects, and Models M10 to M13 scrutinizing deck thickness. Optimization was achieved through a comprehensive analysis encompassing load versus deflection behaviour, end slip, energy-based ductility of the slab and strain characteristics of the profile deck sheet. By systematically varying these parameters across the different models, a nuanced understanding of their impact on structural behaviour and performance has been attained. These insights are pivotal for refining the design and enhancing the overall effectiveness of the profiled deck in structural applications.

3.1.1 Effect of deck height

Finite element analysis revealed a characteristic load versus deflection behaviour of the continuous composite slab exhibiting distinct elastic, yield, and ultimate load regions. In Figure 11 the pronounced deformation profile between the yield point and slab failure is seen. Increasing the deck height from 45 to 70 mm resulted in an initial increase in the load-bearing capacity of the slab as the height increases, peaking at 60 mm height before a subsequent decline in ultimate load. The deeper profile deck facilitated a larger bonding area between the concrete slab and the steel deck, thereby augmenting composite action and load distribution. Consequently, an improved load-bearing capacity was observed up to a certain threshold of height increment. However, beyond 60 mm height, the increased distance between the top and bottom fibers of the slab led to diminished composite action, consequently reducing the ultimate load capacity.

Moreover, the deflection recorded was higher for the model with a 60 mm deck height model M4, indicating superior ductility compared to other models. Figure 12 illustrates higher strain concentrations at the loading points. While the strain in the steel deck may not be exclusively influenced by the profile deck height, a deeper profile deck can enhance anchorage and interaction between the steel and concrete, facilitating more efficient load transfer and potentially reducing strains in the steel components. Hence, model M4, with its higher load capacity of 108.38 kN and lower strain 0.024, will be selected for further investigations.

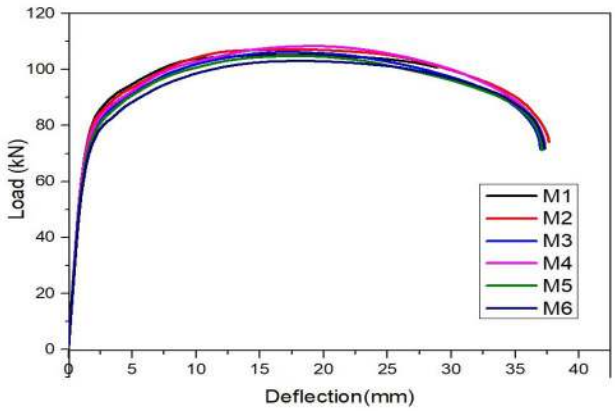


Figure 11 Load Vs. Deflection based on the variation in deck height

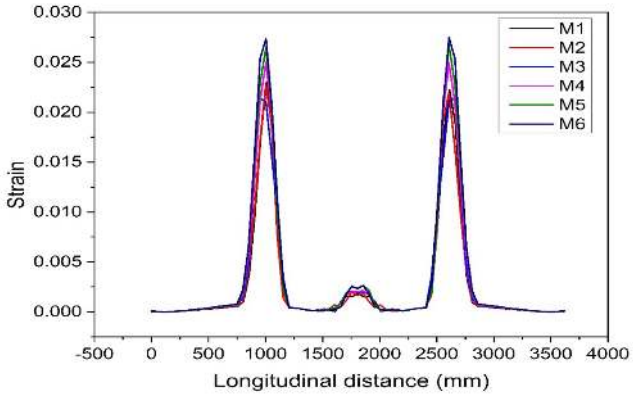


Figure 12 Strain in profile deck sheet based on the variation in deck height

3.1.2 Effect of shear span

The effect of variation of shear span on the performance of the slab is studied and the following results were observed. The Figure 13 represent the load versus deflection characteristics of M4, M7, and M8. Beyond the peak load all curves exhibit a descending trend with M4 displaying the most gradual decline and M8 the sharpest. This post-peak behaviour indicated the response of the slab to loads beyond their maximum capacity potentially suggesting a decrease in stiffness or structural integrity. A steeper decline implies a reduced ability of the slab to support additional load after reaching its peak capacity. Furthermore, it is noteworthy that the ultimate load of M4 surpasses that of M7 by 12.5% and that of M8 by 2.9%. In Figure 14, the peak strain attained distinctly due to change in shear span is shown. The model M4 reaches the highest strain at 0.024, followed by M7 at 0.025, finally M8 at 0.035. Maximum strain is absorbed as load increases and shear span drops from 850 mm to 425 mm. The results indicate that the profile deck with a shear span of 850 mm exhibits a greater load bearing capability and a reduced strain. These findings will be utilised for further research purposes.

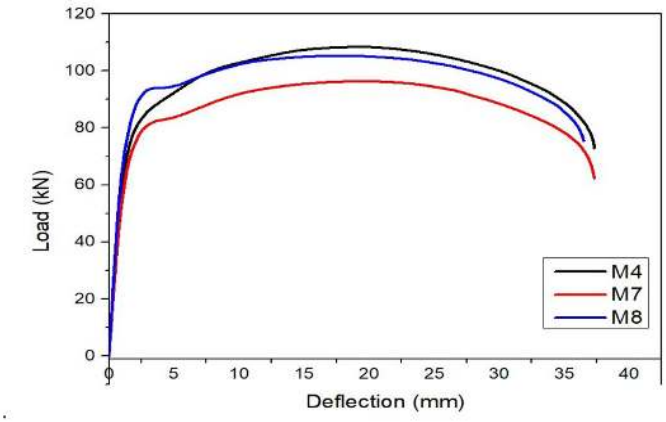


Figure 13 Load Vs. Deflection based on the variation in shear span

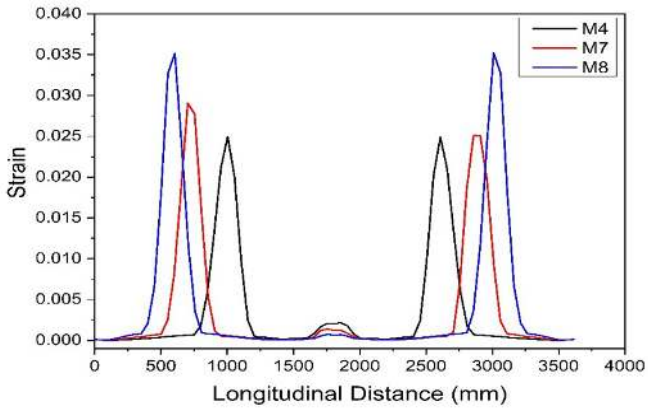


Figure 14 Strain in profile deck sheet based on the variation in shear span

3.1.3 Effect of thickness

The load deflection behaviour of the slab with varying thickness of deck is presented in Figure 15. The structures are unable to carry additional load as deflection increases. The ultimate load-carrying capacity showed an increasing trend with increase in thickness of the deck sheet. The same trend was observed in (Raebel et al., 2020). The model M13 has a load of 123.89 kN which has the thickest deck of 1.2 mm, followed by M12 with an ultimate load of 120.33 kN and down to M4 with a load of 108.38 kN having the thinnest deck. All thicknesses from 0.75 mm to 1.2 mm result in similar strain values at the peaks as in Figure 16, suggesting that within this range the thickness of the deck sheet does not significantly affect the maximum strain experienced by the slab at mid support. Since there is no significant divergence in the strain peaks with increasing thickness it imply that the deck sheet thickness in the range tested has a minimal influence on the elastic behaviour of the slab. Thicker profile deck sheets are more material-intensive, which directly increases the cost and self-weight. To manage the implications effectively setting the thickness of deck sheets to a maximum of 1 mm is proposed for further investigation.

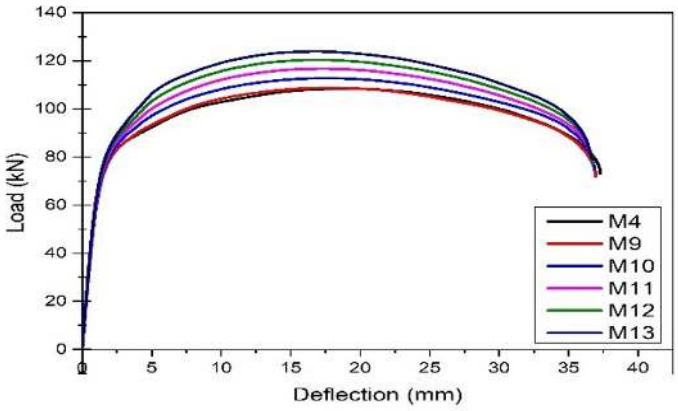


Figure 15 Load Vs. Deflection based on the variation in thickness

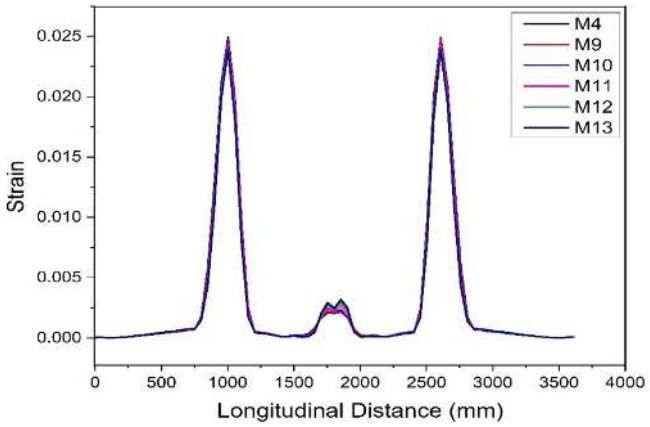


Figure 16 Strain in profile deck sheet based on the variation in thickness

3.1.4 End slip

In a continuous composite slab, end slip refers to the slip between the concrete slab and the steel deck profile caused by differential movement of the two components. This slip can have an impact on the composite slab's structural performance and integrity, particularly in load distribution, stiffness, and overall strength. The end slip in steel-concrete composite continuous slabs is influenced by multiple factors, including deck height, shear span, and deck thickness as shown in Figure 17. As deck height increases from 45 mm in model M1 to 70 mm in model M6, the model M1 and M4 both had same value of end slip of 7.41 mm the bond between the steel and concrete significantly impact end slip. For the models with deck height between 50 mm, 55 mm, and 65 mm display lower end slip values. The end slip decreases as the shear span reduces from 850 mm in M4, 560 mm in M7 and 425 mm in M8 indicating that shorter shear spans could potentially contribute to lower end slip values. This might be attributed to the reduced leverage effect in shorter spans, leading to less slippage at the ends. There is a noticeable trend where increasing deck thickness ranges from 0.8 mm (M9) to 1.2 mm (M13) results in a fluctuation of end slip values and reaching the highest at 1 mm for M11 (7.67 mm). This shows that there might be a complex relationship between deck thickness and end slip, where beyond certain thickness other factors such as the composite action or material properties may dominate the behaviour. The increase in thickness could enhance the stiffness of the slab, potentially affecting the bond and slip characteristics. However, the highest slip at an intermediate thickness (1 mm for M11) indicates that blindly increasing thickness does not linearly decrease end slip highlighting the importance of optimizing thickness for both structural performance and material efficiency. All the specimens passed the definition of ductility as per EC4 (EN, 1994) i.e. load at the peak is more than 10% of the load causing 0.1mm slip. Altogether, the end slip of composite slabs is influenced by a complex interplay of deck height, shear span, and deck thickness. Optimal performance in terms of minimizing end slip likely depends on achieving a balanced design that considers the interactions between these parameters.

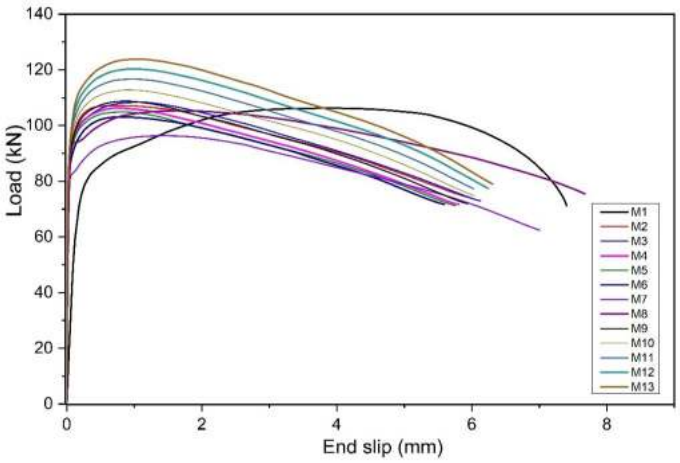


Figure 17 End slip with respect to ultimate load

3.1.5 Energy based ductility

Energy-based ductility in composite slabs refers to the capacity of a composite slab system to deform under loading beyond its elastic limit without a significant loss of strength. The energy-based ductility variation dependent on deck height, shear span, and deck thickness is depicted in Figure 18. The energy absorption values of models M1 through M6, with deck heights ranging from 45 mm to 70 mm, exhibit a consistent upward trend as the deck height increases. This suggests that slabs with higher deck heights may have a better capacity to absorb energy, as the additional depth allows for a larger amount of material to distribute and absorb energy under loading. When comparing M4 to M7 and M8, the larger shear span of M4 might allow for more flexibility and energy absorption before failure. However, this impact also depends on the additional factors, such as deck height and thickness. The models M9 to M13 exhibit a definite pattern of escalating energy absorption as the deck thickness increases. This pattern indicates that increasing the thickness of decks improves the energy absorption capacity of composite slabs by increasing the volume and stiffness of the material. This in turn enhances the overall structural resilience against applied forces. The structural capacity to absorb energy is a crucial factor in the design and performance of composite slabs when subjected to dynamic and static loads. Each of these elements has a significant role in determining this capacity. This observation has the potential to inform the enhancement of composite slab design for applications. Hence assuring the attainment of sufficient energy absorption capabilities to fulfil performance criteria.

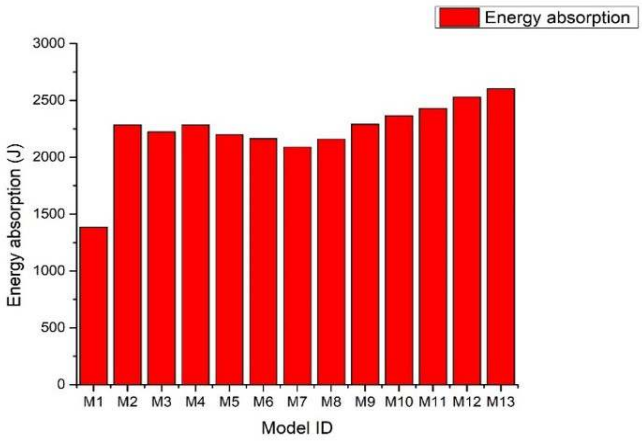


Figure 18 Energy based ductility variation

3.2 Optimization of CFRP

3.2.1 Effect of length

Two lengths of CFRP wrapping i.e. 1.7 m and 1.4 m are employed and the variation is shown in Figure 19(a). The model CF1 with a CFRP wrapping length of 1.7 meters, exhibits a 53.73% lower deflection compared to CF2 slab with shorter length CFRP. The CF2's shorter length demonstrates a lesser load capacity of 21.09% compared to CF1's. The

reduced deflection and increased load capacity of CF1 suggest that a longer CFRP strip length contributes positively to the slab's stiffness and structural integrity. The additional length provides more effective distribution of forces and enhances the slab's ability to resist bending deformation under load. When the CFRP is placed in limited width three strips spaced equally along the width the model CF3 with longer strips shows 46.67% less deflection and a 26.62% increase in load capacity compared to CF4. Alike the first comparison, the performance of CF3 reinforces the idea that increased length and strategic placement of CFRP strips can significantly enhance the load-bearing capacity and reduce the deflection of the slab. The equal spacing between the CFRP strips ensures a balanced distribution of the load across the slab improving its overall stiffness and resistance to deformation. Both the model CF6 and CF8 have a single CFRP strip placed at the centre shows a deflection of 18.43 mm and a higher load capacity of 109.87 kN compared to CF8 with deflection of 15.60 mm, load capacity of 80.13 kN. This indicates an opposite trend to the previous comparisons. Although the length of the CFRP strip does affect the load-bearing capacity, the observed trend indicates that the location and probably the quality of the concrete slab itself are more important factors in determining the deflection of the slab under load. The potential efficacy of centrally positioning the strip in mitigating deflection may be comparatively lower than that of an equally spaced technique, suggesting a multifaceted interplay between strip length, location, and slab reaction. CF7 and CF9, which have two layers of CFRP strips positioned at the center, exhibit enhanced load capacity as their length increases. However, they also have a subtle deflection reaction, comparable to CF6 and CF8. This configuration implies that the incorporation of extra layers of CFRP might augment the load-bearing capability is because of the augmented thickness and rigidity offered by the supplementary layer. Nevertheless, the analysis of deflection response reveals that the mere addition of additional layers or extension of the CFRP does not provide a direct reduction in deflection. As in Figure 19 (b), a longer CFRP strip (1.7 m) results in a lower strain implying better distribution of stress or more effective reinforcement over a larger area.

The structural performance of composite slabs is substantially influenced by the length and strategic positioning of CFRP strips. Extended CFRP strips, particularly when strategically positioned or layered, tend to improve the ability to bear loads while also affecting the patterns of deflection in intricate manners. This highlights the need of using a comprehensive methodology when developing CFRP reinforcements, considering several parameters such strip length, positioning, and stacking, to get the most efficient structural performance.

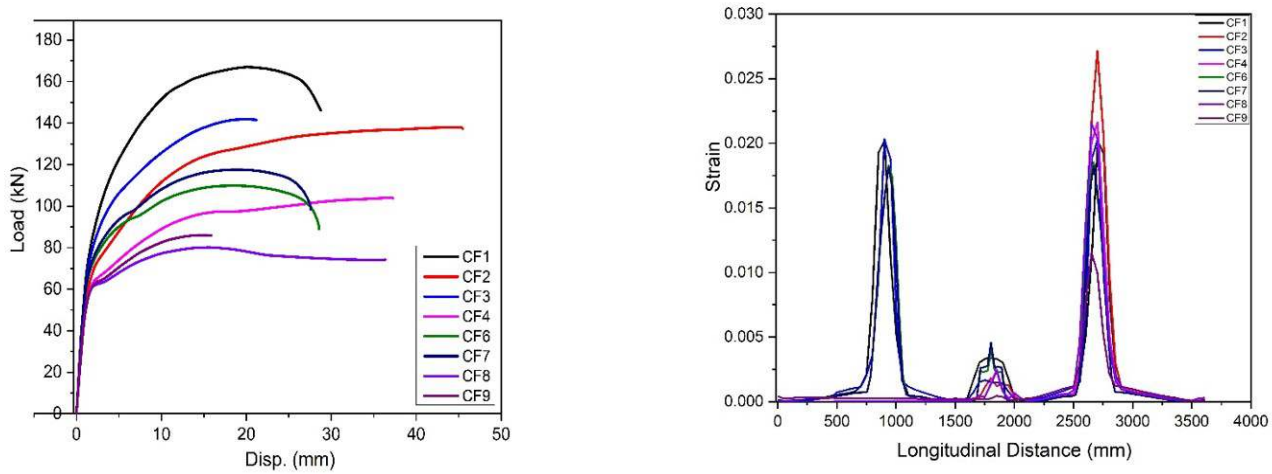


Figure 19 *Effect of length of CFRP (a) Load vs. Deflection (b) Strain in deck slab*

3.2.2 Effect of layers

Figure 20 (a) illustrates the impact of CFRP layers inside the hogging area of the composite continuous slab on load-deflection. The CF6 model uses a single layer of CFRP and demonstrates a displacement of 18.43 mm when subjected to a load of 109.87 kN. The provided data illustrates the initial performance of a single-layer reinforcement with a length of 1.7 m. The CF7 model incorporates two layers of CFRP, resulting in a marginal displacement increase of 2.72% compared to the CF6 model. This observation indicates a little reduction in stiffness. Nevertheless, the load capacity experiences a

substantial enhancement with a 7.04% rise, signifying an improvement in strength attributed to the inclusion of an extra layer. The CF8 type, including a single layer of CFRP, exhibits a displacement of 15.60 mm when subjected to a force of 80.13 kN. The shorter 1.4 m strips are based on a single-layer baseline. The CF9 model has a twofold increase in layers and a displacement reduction of 4.09% compared to the CF8 model, indicating an enhancement in stiffness resulting from the inclusion of the additional layer. The load capacity is raised by 7.40% due to the double layering, which provides greater strength equivalent to the 1.7 m strips, while also offering the advantage of higher stiffness.

The load capacity at both lengths (1.7 m and 1.4 m) is consistently enhanced by an increase in CFRP layers, highlighting the strengthening impact of additional CFRP layer. Adding additional layers to 1.7 m CFRP strips results in minimal displacement, indicating a slightly flexible system. Adding extra layers to 1.4 m CFRP strips reduces displacement, indicating a more rigid slab. The load capacity increases proportionally with the addition of a second CFRP layer, resulting in an approximate improvement of 7%. Figure 20 (b) demonstrates that the use of two layers of CFRP exhibits superior strain reduction and distribution capabilities compared to a single layer. In models with shorter length of CFRP, the efficacy of the two-layer system is more evident in comparison to the 1.7 m models. Utilising two layers of shorter CFRP strips might be advantageous when prioritising stiffness, particularly in seismic zones. On the other hand, if the objective is to optimise load capacity while minimising displacement, it may be more advantageous to utilise two layers on the longer strips.

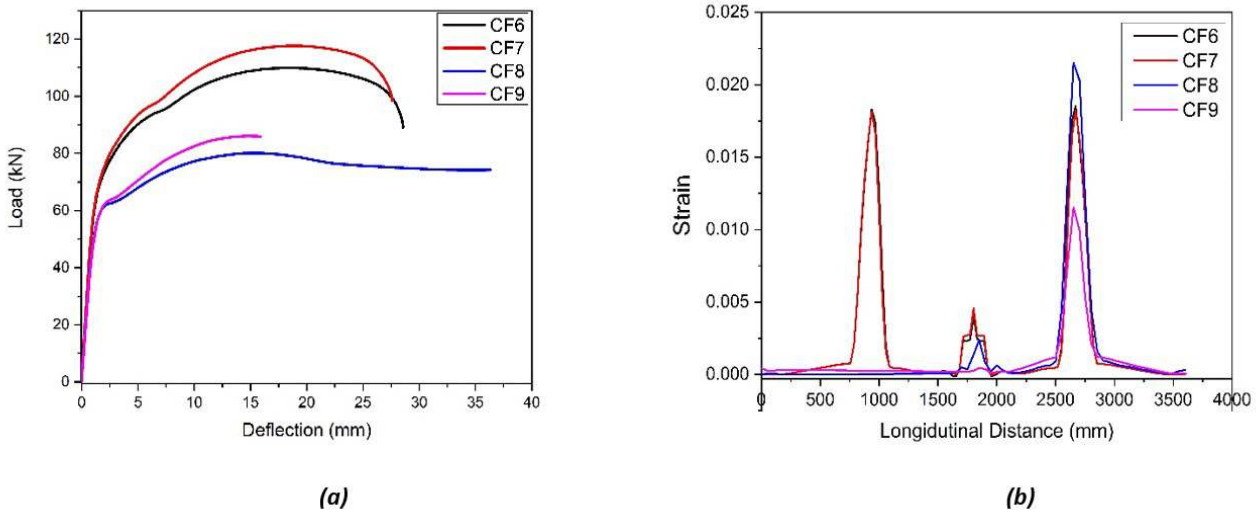


Figure 20 *Effect of layers of CFRP (a) Load vs. Deflection (b) Strain in deck slab*

3.2.3 Effect of width

When comparing the CFRP wrapping of full width and strips of 1.7 m length as in Figure 21 (a), CF1 has the highest load capacity of 167.04 kN with a highest displacement of 20.04 mm indicating that wrapping the entire width increases load capacity and flexibility of the slab. The model CF3, with three strips had a reduction in load capacity of 17.7% and model tend be stiffer than CF1. This suggests that using multiple strips along the width balances load capacity and stiffness. The model CF6, with a single strip has the lowest load capacity of 109.88 kN and a displacement of 18.43 mm, showing that a single strip at the centre provides a stiffer system with less load capacity. CF1 exhibits similar trend in strain distribution with CF3 due to the continuous support across the full width. However, CF3 had higher strain as shown in Figure 21 (b). The model CF6, with central placement had the better strain reduction.

When comparing the CFRP wrapping of full width and strips of 1.4 m length, CF2 has the highest load capacity of 137.94 kN and the highest displacement of 43.30 mm from which it is evident that CFRP strengthening of full-width wrapping provides high load capacity at the expense of higher ductility. The model CF4 with three strips provides better load capacity than a single strip at centre and had a higher displacement of 36.98 mm. While CF8 has the least displacement of 15.61 mm indicating the higher stiffness similar to the trend noted in 1.7 m length CFRP. When studying the strain behaviour, it is seen that CF2 has a higher peak strain than CF4 and CF8 which suggests that for shorter length of CFRP strengthening distributing CFRP in limited width either as multiple strips or a single central strip is more beneficial than a full-width application.

When comparing CFRP wrapping of mixed length in two layers CF5 has two layers of mixed-length strips placed at centre providing a load capacity and displacement suggesting a balance between stiffness and load capacity. CF10 with three strips spread across the width and two layers shows higher stiffness (lowest displacement) and a good load capacity (140.06 kN), possibly the best balance among the three. CF11, like the previous full-width models, shows the highest load capacity (176.77 kN) and the highest displacement (20.88 mm), meaning that despite being the most flexible, it can carry the highest load. CF10 as having the lowest peak, indicating the most effective strain reduction due to the combination of multiple strips and two layers. CF11 and CF5 would show higher strain values, with CF11 potentially showing a more evenly distributed strain across the width than CF5 due to the full-width wrap. The distribution of CFRP (whether by multiple strips or full-width) and the number of layers plays a significant role in the strain characteristics of the slabs. Multiple strips and additional layers tend to reduce and more evenly distribute strain.

Overall, CFRP wrapping width and layering markedly influence load capacity and structural flexibility. Full-width wraps consistently achieve higher load capacities with increased flexibility. In contrast, single-strip placements maximize stiffness but at the expense of load capacity. Multiple-strip configurations and layering strategies offer balanced solutions, adapting load support to displacement characteristics for optimal structural reinforcement.

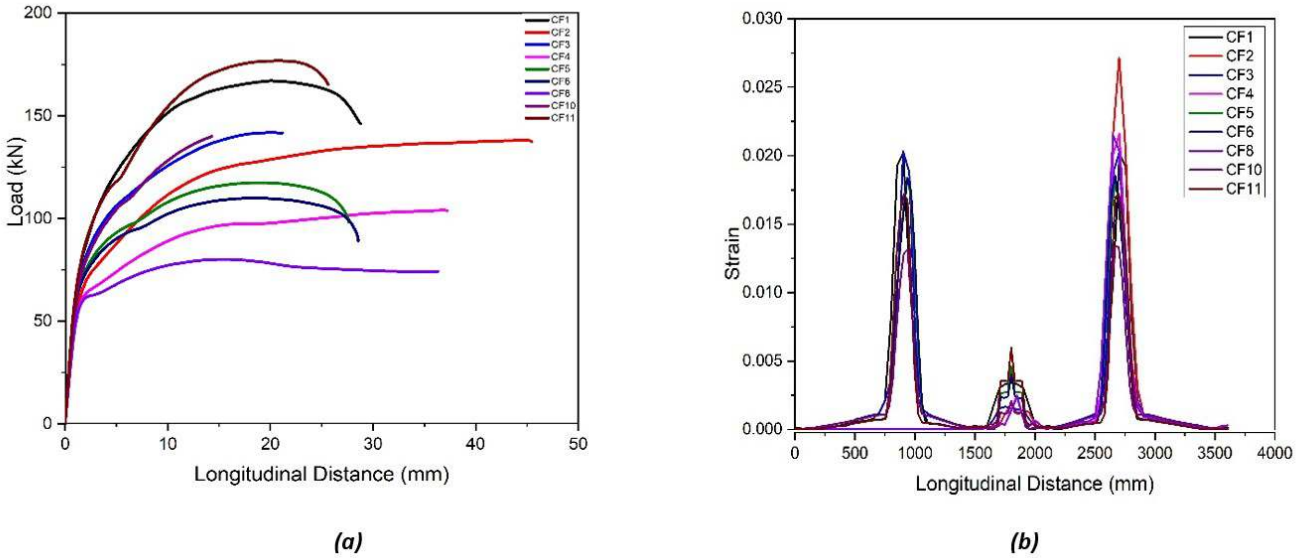


Figure 21 Effect of width of CFRP (a) Load vs. Deflection (b) Strain in deck slab

3.2.4 End slip of slabs with CFRP reinforcement

In Figure 22, the load increases with end slip up to a specific level for each CFRP configuration before either reaching plateau or exhibiting a downward trend, which indicates the maximum load that the configuration can sustain before failure. In terms of load transfer and CFRP efficiency, models that have smaller end slips at higher loads perform superior. The full width CFRP CF2 demonstrates a 52.04% increase in end slip compared to CF1, indicating that slabs with shorter CFRP lengths may encounter greater slip prior to reaching their performance threshold, owing to enhanced flexibility. CF3 has a lower end slip in evenly spaced strips compared to CF4, measuring 1.92 mm and 7.14 mm respectively. This suggests that the slab with a longer CFRP strip effectively limits slip by enhancing load distribution. CF5 and CF7 have comparable end slip values of 5.21 mm and 5.18 mm, respectively, in their two layered configurations. The model CF9 has a significantly reduced slip of 3.25 mm, indicating that the benefits of a two-layer system are contingent upon the specific design. CF6 and CF8 exhibit different end slips of 5.4 mm and 7.89 mm respectively for single layered strips. The latter has a larger value, suggesting that the shorter length of CFRP has an impact on end slip. When two strips of various lengths are used together, CF10 demonstrates exceptional performance with a minimal end slip of 1.27 mm. This demonstrates an optimal equilibrium between slip resistance and load-bearing capacity, achieved via the use of both length variations and layering techniques.

The findings indicate that the slip characteristics are considerably influenced by the interplay of CFRP length, breadth, and layering complexity. There is a propensity for increased slip in both full-width and strip applications observed in models with shorter CFRP lengths. In contrast, designs using spaced strips present a compromise between load capacity and slip. However, it is important to note that this equilibrium is significantly impacted by the design and application of the CFRP layers.

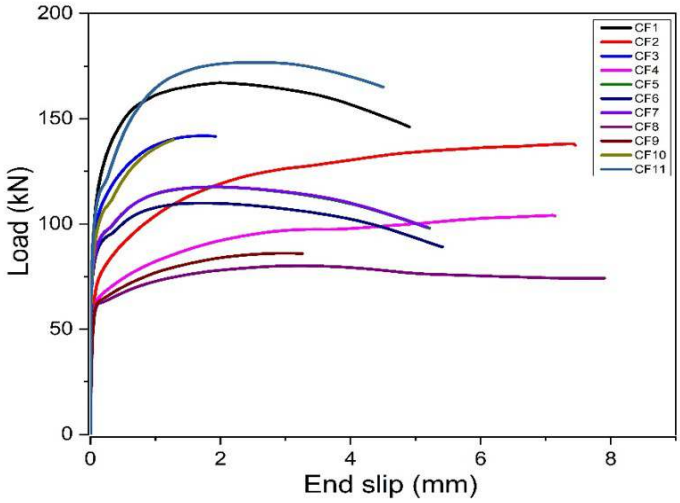


Figure 22 End slip of slabs with CFRP reinforcement

3.2.5 Energy based ductility of slabs with CFRP reinforcement

The energy-based ductility is displayed in Figure 23, and the length, breadth, and number of CFRP layers are compared. CFRP strips with shorter lengths often exhibit more energy absorption. This is apparent when comparing CF2, which has an energy that is 16.43% higher than CF1, and similarly, CF4, which has an energy that is 46.36% more than CF3. The potential reason for the heightened energy absorption seen in shorter strips might be attributed to the elevated stress concentration over the decreased length. The energy absorption of models with two layers, namely CF5, CF7, and CF10, is seen to be greater compared to those with only one layer. The energy absorption of full-width CFRP wraps CF1 and CF2 exhibits a notable disparity, which can be attributed to the length of the strip. Models including evenly dispersed strips CF3 and CF4 exhibit lower energy absorption compared to the full-width wraps. This suggests that a concentrated application of CFRP over the entire width is more efficient in terms of energy absorption than using distributed strips. For example, the CF11 model has a 30.5% higher energy absorption capacity in comparison to the CF10 model, hence enhancing the efficacy of full-width wraps.

The length of CFRP significantly impacts its energy absorption capability, with shorter strips exhibiting superior performance. The introduction of additional layers is known to improve energy absorption. However, it is crucial to consider the potential interaction with other elements, such as the location of strips. Full-width carbon fibre reinforced polymer (CFRP) wraps, particularly when including many layers, exhibit greater efficacy in terms of energy absorption as compared to arrangements where strips are dispersed throughout the width of the slab.

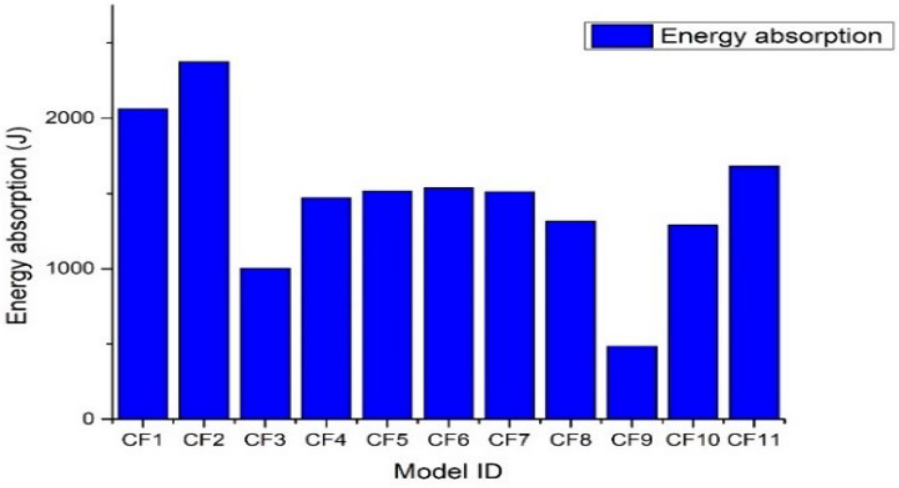


Figure 23 Energy based ductility variation of slabs with CFRP reinforcement

4. THEORETICAL METHOD

To ascertain the ultimate load of the composite slabs, utilise the strain correlation and force equilibrium criteria(Hosen et al., 2015), as shown in Figures 24(a) and (b). In order to obtain the ultimate moment of composite slab strengthened with CFRP, the forces in tension as well as compression is calculated separated using the stress variation diagram as in Figure 24. In addition, to conventional composite slab, additionally the force resistance of CFRP is calculated. Using the equilibrium of forces between tension and compression, the depth of neutral axis (a) is calculated. The ultimate moment is calculated by the product of force of each component and corresponding lever arm distance from both tension and compression region. The expected failure of the reinforced beam is due to the compression concrete crushing after the tension reinforcement yields. In the constant moment zone, the computation is performed**.** In the event of failure, the forces P_c, P_t and P_{cfrp} are represented by the following Equation (3) – (6).

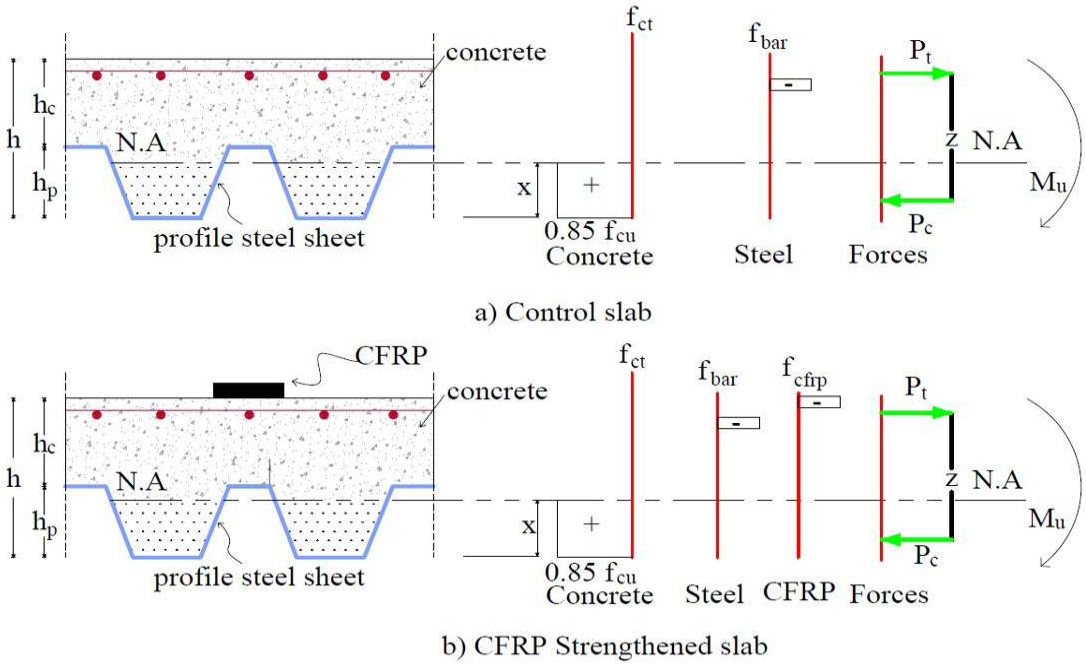


Figure 24 Flexural stress variation across composite slab

$P_c = 0.67 f_{cu}$ (3)

$P_s = A_s F_y$ (4)

$P_{cfrp} = A_{cfrp} E_{cfrp} \epsilon_{cfrp}$ (5)

ϵ_{cfrp} is calculated by $\epsilon_{cfrp} = \epsilon c \frac{d_{Cfrp} - x}{x}$ (6)

The equilibrium of forces results in the subsequent relationship:

$$\mathbf{0.67 b f_{cu} x^2 + \left(\epsilon_{cfrp}\, E_{cfrp} A_{cfrp} - A_s F_y\right) x - \epsilon_c\, E_{cfrp} A_{cfrp} d_{cfrp} = 0} \quad (7)$$

The determination of the depth of the neutral axis (x) is achieved by utilising Equation (7)

Calculation of ultimate bending moment is determined by the following Equation (8)

$$\mathbf{M_u = A_s F_y \left(d_s - \frac{x}{2}\right) + E_{cfr} A_{cfrp}\, \epsilon_c \frac{(d_{cfrp} - x)}{x} \left(d_{cfrp} - \frac{x}{2}\right)} \quad (8)$$

Predicting the ultimate load of test specimens was based on equilibrium conditions. The ultimate load P is calculated from Equation (9)

$$P = \frac{2M_u}{L_a} \quad (9)$$

Where,
b - Width of composite slab
h - Overall depth of the composite slab
d_s - Distance between the centre of gravity of the tension steel bars and the bottom fiber of the concrete
d_{cfrp} - Distance between the bottom fiber of concrete and the centre of gravity of the CFRP reinforcement
x - Depth of neutral axis
ϵ_c - Strain of the bottom fiber of concrete
ϵ_{cfrp} - Strain CFRP
A_{cfrp}- Area of CFRP used for strengthening of the slab
E_{cfrp} - Young's modulus of the CFRP
F_y - Yield strength of the profile deck sheet
A_s - Area of the tension reinforcement
F_{cu} - Compressive strength of concrete
M_u - Ultimate moment of slab
P - Ultimate load of slab
L - Length of the slab
P_c - Total compressive force in concrete
P_s -Total tensile force in steel
P_{cfrp} -Total tensile force in CFRP

(Dahham et al., 2018) studied the behavior of continuous composite slab strengthened with CFRP laminates. The study involved experiment on four specimens of which three were strengthened in the hogging region using a single strip of CFRP of varying length and a control specimen with no strengthening. The theoretical method was applied to the above study and ultimate moment of the slabs was calculated. It has been observed that from experimental moment values for specimen strengthened with CFRP of 1, 1.4 and 1.7m CFRP were 23, 25.8 and 27.9 kNm respectively. The predicted value for all slabs using the theoretical method was found to be 21.5 kNm since the effect of length of CFRP is not included in the theoretical calculation. Hence, all the slabs had same predicted value. The results of the proposed equations are having a good agreement with experimental results with a minimum discrepancy of 6.9%. The comparison between FE models and predicted results from theoretical approach of ultimate load as shown in Figure 25. The values of ultimate load predicted using the above method showed similar value obtained from the FE analysis for models CF4 and CF6 with a difference of less than 5%. For the models CFRP strengthen across the full width slabs the predicted value surpasses the FE model values by 29.9%. It depicted that the prediction has good aggreement with FE analysis in the case of CFRP with single layer strips. When it comes to two layers of CFRP, there is a slight change in neutral axis due to addition of another layer of CFRP component. Because of this, there is a change in internal force and stress distribution. In case of full width strengthened slab, the slab width directly affect the bending stiffness. The bending stiffness increases with increase in width of CFRP. Hence, there is a small discrepancy in CF1 and CF2. Altogether, there is a good agreement between predicted and FE results.

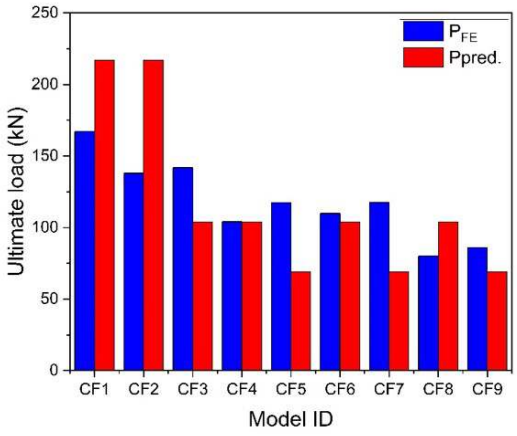


Figure 25 Ultimate load variation between FE analysis and Prediction method

5. CONCLUSION

The conclusive insights drawn from this study underscore the pivotal role of geometric optimization in enhancing the structural integrity and performance of profiled deck systems. By employing finite element analysis with great attention to detail, this study has elucidated the impact of differing deck height, thickness, and shear span on the load-bearing capacity and resilience of the composite slab. The current investigation offers a comprehensive framework for comprehending the interconnectedness of design elements and their combined influence on structural performance. The work has been extended to provide a detailed examination of the use of Carbon Fiber Reinforced Polymer (CFRP) as a strengthening external reinforcement. It has revealed the complex relationship between the configuration of CFRP, the elements of the slab, and its performance. By conducting a meticulous analysis of the load-versus-end slip characteristics in different models, crucial elements that significantly influence the effectiveness of CFRP as a reinforcing material was discovered. The criteria encompassed in this analysis are the length of the CFRP strips, the quantity and arrangement of layers, and the degree of application breadth. The findings provide valuable recommendations for enhancing structural design of continuous composite slab using CFRP in the hogging region.

1. In general, the overall structural performance of the slab is improved when Carbon Fiber Reinforced Polymer (CFRP) is applied using the surface-mounted approach to strengthen slabs in the hogging region. In the comparison of conventional composite slab with optimized profiled deck M11 and CFRP strengthened slab CF11's the ultimate load and maximum displacement of are 51.5% and 21.32% higher than M11 respectively. However, the ductility decreased of the strengthened slabs compared to the control slab.
2. Parametric evaluations of models M1 to M13 showed that deck height, thickness, and shear span significantly affect slab load-bearing efficiency. As deck height increased, the ultimate load capacity and ductility increased peaking at 60 mm height before a subsequent decline in ultimate load.
3. The findings indicate that increasing the shear span, as shown in models M7 and M8, has several benefits. There a more favourable distribution of stresses across the slab, resulting in enhanced stability and strength. Of the three shear spans 850 mm is found to have nearly 12% higher load carrying capacity compare to other spans.
4. As the thickness increased (0.75 mm to 1.2 mm), the ultimate load carrying capacity has increased. The ultimate load of M11(1.2 mm thick) is 14.31% higher than M4(0.75 mm thick). Thicker profile deck sheets are more material-intensive, which directly increases the cost and self-weight. To manage the implications effectively, setting the thickness of deck sheets to a maximum of 1 mm is proposed for the present study.
5. The careful assessment of the variance in CFRP application, including factors such as length, width, and the number of layers, was conducted. The CF1(1.7 m) and CF2(1.4) models, which differ in the length of CFRP, depicted the importance of CFRP coverage enhances the strength and ductility of the slab.
6. In comparing the models of different length of CFRP, CFRP of 1.7 m length is 21.09%, 36.28%, 37.12% and 36.67% higher than 1.4 m length in terms of full width, three strips, one strip and one strip two layers respectively. In terms of the number of layers, C7 is 7.04% higher than C6, while C8 is 7.4% higher than C9. In terms of width, its obvious that full width has the maximum load carrying capacity of 176.78 kN. The analysis of models CF3 and CF4, CF6 and CF8, and CF7 and CF9 offered a distinct viewpoint on the optimum number of CFRP strips and their strategic positioning. The implementation of a layered approach in models CF6, CF10, and CF11, which incorporate numerous layers of CFRP, highlights the advantages of layering in strengthening the slabs. This is supported by the significant improvements observed in the ultimate load capacity and energy-based ductility indices.
7. The theoretical approach was developed to predict the ultimate load of the continuous composite slab strengthened with CFRP. The method tends to overestimate the capacity of the slab when it is strengthened fully across the width. The prediction was accurate for models with one central strip of both longer and shorter length of CFRP.
8. In conclusion, the findings of this analytical endeavour highlight the significant advantages of customising deck shape and using CFRP reinforcement. These enhancements not only amplify the load-bearing capacity of composite slabs but also introduce additional resilience, indicating that such modifications can lead to significant advancements in the design and construction of structural components. Further investigation is necessary to authenticate these finite element model results to examine the enduring performance of CFRP-reinforced slabs when subjected to dynamic stress and fluctuating environmental circumstances.

Author's Contribuitions: Conceptualization, Karthiga.S and Umamaheswari.N; Investigation, Karthiga.S and Umamaheswari.N; Writing - original draft, Karthiga.S; Writing - review & editing, Umamaheswari.N;

Editor: Rogério José Marczak

References

Abas, F. M., Gilbert, R. I., Foster, S. J., & Bradford, M. A. (2013). Strength and serviceability of continuous composite slabs with deep trapezoidal steel decking and steel fibre reinforced concrete. *Engineering Structures, 49*, 866–875. https://doi.org/10.1016/j.engstruct.2012.12.043

Abdullah, R., & Samuel Easterling, W. (2009). New evaluation and modeling procedure for horizontal shear bond in composite slabs. *Journal of Constructional Steel Research, 65*(4), 891–899. https://doi.org/10.1016/J.JCSR.2008.10.009

Abdulrazzaq, M. M., Hilo, S. J., Sabih, S. M., Hilmi, S. A., Al-Zand, A. W., & Ali, M. M. (2022). Numerical investigation for the flexural load behaviour of profiled composite slab strengthened with CFRP. *Materials Today: Proceedings, 61*(xxxx), 1115–1125. https://doi.org/10.1016/j.matpr.2021.10.513.

Anil, Ö., Kaya, N., & Arslan, O. (2013). Strengthening of one way RC slab with opening using CFRP strips. *Construction and Building Materials, 48*, 883–893. https://doi.org/10.1016/J.CONBUILDMAT.2013.07.093

Bank, L. C., & Arora, D. (2007). Analysis of RC beams strengthened with mechanically fastened FRP (MF-FRP) strips. *Composite Structures, 79*(2), 180–191. https://doi.org/10.1016/J.COMPSTRUCT.2005.12.001

Cifuentes, H., & Medina, F. (2013). Experimental study on shear bond behavior of composite slabs according to Eurocode 4. *Journal of Constructional Steel Research, 82*, 99–110. https://doi.org/10.1016/J.JCSR.2012.12.009

Congro, M., Monteiro, V. M. de A., Brandão, A. L. T., Santos, B. F. do., Roehl, D., & Silva, F. de A. (2021). Prediction of the residual flexural strength of fiber reinforced concrete using artificial neural networks. *Construction and Building Materials, 303*. https://doi.org/10.1016/j.conbuildmat.2021.124502

Crisinel, M., & Marimon, F. (2004). A new simplified method for the design of composite slabs. *Journal of Constructional Steel Research, 60*(3–5), 481–491. https://doi.org/10.1016/S0143-974X(03)00125-1

Dahham, K. W., Baharom, S., Badaruzzaman, W. H. W., Muhammad, N., & Al-Zand, A. W. (2018). Static structural performance of continuous composite slab strengthened by cfrp laminate in the hogging moment region. *Journal of Engineering Science and Technology, 13*(6), 1489–1499.

Dalfré, G. M., & Barros, J. A. O. (2013). NSM technique to increase the load carrying capacity of continuous RC slabs. *Engineering Structures, 56*, 137–153. https://doi.org/10.1016/J.ENGSTRUCT.2013.04.021

de Andrade, S. A. L., Vellasco, P. C. G. d. S., da Silva, J. G. S., & Takey, T. H. (2004). Standardized composite slab systems for building constructions. *Journal of Constructional Steel Research, 60*(3), 493–524. https://doi.org/10.1016/S0143-974X(03)00126-3

Daniels, B. J. and Crisinel, M., "Composite Slab Behavior and Strength Analysis. Part II: Comparisons with Test Results and Parametric Analysis," J. Struct. Eng., vol. 119, no. 1, pp. 36–49, Jan. 1993, doi: 10.1061/(ASCE)0733-9445(1993)119:1(36).

Deng, J., Lee, M. M. K., & Li, S. (2011). Flexural strength of steel–concrete composite beams reinforced with a prestressed CFRP plate. *Construction and Building Materials, 25*(1), 379–384. https://doi.org/10.1016/J.CONBUILDMAT.2010.06.015

Diab, H. M. A., Abdelaleem, T., & Rashwan, M. M. M. (2020). Moment redistribution and flexural performance of RC continuous T-beams strengthened with NSM FRP or steel bars. *Structures, 28*, 1516–1538. https://doi.org/10.1016/J.ISTRUC.2020.09.003

El-Zohairy, A., Salim, H., Shaaban, H., Mustafa, S., & El-Shihy, A. (2017). Experimental and FE parametric study on continuous steel-concrete composite beams strengthened with CFRP laminates. In *Construction and Building Materials* (Vol. 157, pp. 885–898). Elsevier. https://doi.org/10.1016/j.conbuildmat.2017.09.148

EN, B. S. (1994). 1-1: 2004: Eurocode 4. Design of composite steel and concrete structures. General rules and rules for buildings. In *British Standards Institution, London*.

Faust, T. (1997). Lightweight Concrete in Composite Structures. *Institut Fur Massivbau Und Baustofftechnologie, Universitat Leipzig, LACER, 2*.

Ferrer, M., Marimon, F., & Crisinel, M. (2006). Designing cold-formed steel sheets for composite slabs: An experimentally validated FEM approach to slip failure mechanics. *Thin-Walled Structures, 44*(12), 1261–1271. https://doi.org/10.1016/J.TWS.2007.01.010

Florides, M. M., & Cashell, K. A. (2017). Numerical Modelling of Composite Floor Slabs Subject to Large Deflections. *Structures, 9*, 112–122. https://doi.org/10.1016/j.istruc.2016.10.003

Gholamhoseini, A. (2018). Experimental and finite element study of ultimate strength of continuous composite concrete slabs with steel decking. *International Journal of Advanced Structural Engineering, 10*(1), 85–97. https://doi.org/10.1007/s40091-018-0183-3

Gholamhoseini, A., Gilbert, R. I., & Bradford, M. (2018). Long-term behavior of continuous composite concrete slabs with steel decking. *ACI Structural Journal, 115*(2), 439–449. https://doi.org/10.14359/51701133

Gholamhoseini, A., Khanlou, A., MacRae, G., Scott, A., Hicks, S., & Leon, R. (2016). An experimental study on strength and serviceability of reinforced and steel fibre reinforced concrete (SFRC) continuous composite slabs. *Engineering Structures, 114*, 171–180. https://doi.org/10.1016/j.engstruct.2016.02.010

Hibbitt, K., & Sorensen. (2001). *User's Manual, no. v. 3. in ABAQUS/Standard* (Issue v. 3). Hibbitt, Karlsson \& Sorensen. https://books.google.co.in/books?id=Lq7gAAAAMAAJ

Hibbitt, K., & Sorensen. (2019). *User's Manual, no. v. 8*. in *ABAQUS*/Standard. In *Αγαη* (Vol. 8, Issue 5). https://books.google.co.in/books?id=Lq7gAAAAMAAJ

Hofmeyer, H., Kerstens, J. G. M., Snijder, H. H., & Bakker, M. C. M. (2002). Combined web crippling and bending moment failure of first-generation trapezoidal steel sheeting. *Journal of Constructional Steel Research, 58*(12), 1509–1529. https://doi.org/10.1016/S0143-974X(02)00004-4

Hosen, M. A., Jumaat, M. Z., & Islam, A. B. M. S. (2015). Side Near Surface Mounted (SNSM) technique for flexural enhancement of RC beams. *Materials and Design, 83*, 587–597. https://doi.org/10.1016/j.matdes.2015.06.035

Hossain, K. M. A., Attarde, S., & Anwar, M. S. (2019). Finite element modelling of profiled steel deck composite slab system with engineered cementitious composite under monotonic loading. *Engineering Structures, 186*(March 2018), 13–25. https://doi.org/10.1016/j.engstruct.2019.02.008

Houssam, T., Meng, H., & Elhem, G. (2012). Interfacial Bond Strength Characteristics of FRP and RC Substrate. *Journal of Composites for Construction, 16*(1), 35–46. https://doi.org/10.1061/(ASCE)CC.1943-5614.0000236

J. D. Ríos, H. Cifuentes, A. M. La Concha, and F. Medina-reguera (2017), "Numerical modelling of the shear-bond behaviour of composite slabs in four and six-point bending tests," 133, pp. 91–104, doi: 10.1016/j.engstruct.2016.12.025.

Jeeho, L., & Gregory L., F. (1998). Plastic-damage model for cyclic loading of concrete structures. *Journal of Engineering Mechanics, 124*(8), 892–900.

John, K., Ashraf, M., Weiss, M., & Al-Ameri, R. (2022). Parametric finite element study of novel corrugated steel deck for two-way action in steel-concrete composite floors. *Structures, 44*(June), 1152–1167. https://doi.org/10.1016/j.istruc.2022.08.072

Johnson, R. P., & Lee, L.-H. (1977). Composite Structures of Steel and Concrete, Vol. 1. In *Journal of Engineering Materials and Technology* (Vol. 99, Issue 2). https://doi.org/10.1115/1.3443434

Karimipanah, A., Zeynalian, M., & Ataei, A. (2024). Structural Performance of Cold Formed Steel Composite Beams with Profiled Steel Sheeting. *International Journal of Civil Engineering, 2*. https://doi.org/10.1007/s40999-024-00949-2

Kazem, H., Rizkalla, S., & Kobayashi, A. (2018). Shear strengthening of steel plates using small-diameter CFRP strands. *Composite Structures, 184*, 78–91. https://doi.org/10.1016/J.COMPSTRUCT.2017.09.094

Li-Xiang, S., Peng-Zhen, L., Zi-Jiang, Y., Ying-Long, L., & Qu, S. (2021). Experimental study on flexural behavior of gfrp reinforced concrete slabs. *IOP Conference Series: Earth and Environmental Science, 676*(1). https://doi.org/10.1088/1755-1315/676/1/012060

Li, J., Xie, J., Liu, F., & Lu, Z. (2019). A critical review and assessment for FRP-concrete bond systems with epoxy resin exposed to chloride environments. *Composite Structures, 229*, 111372. https://doi.org/10.1016/J.COMPSTRUCT.2019.111372

Lin, W., Yoda, T., & Taniguchi, N. (2014). Application of SFRC in steel–concrete composite beams subjected to hogging moment. *Journal of Constructional Steel Research, 101*, 175–183. https://doi.org/10.1016/J.JCSR.2014.05.008

Liu, X., Tang, L., Jing, Y., Xiang, J., Tian, X., Liu, W., Huang, Y., Zhang, G., Zhao, W., & Yang, G. (2022). Behaviour of continuous steel–concrete composite beams strengthened with CFRP sheets at hogging-moment region. *Composite Structures, 291*, 115695. https://doi.org/10.1016/J.COMPSTRUCT.2022.115695

Lubliner, J. (2008). *Plasticity theory.* Courier Corporation.

Makelainen, P., & Sun, Y. (1998). Development of a new profiled steel sheeting for composite slabs. *Journal of Constructional Steel Research, 46*(1–3), 220. https://doi.org/10.1016/S0143-974X(98)80021-7

Marimuthu, V., Seetharaman, S., Jayachandran, S. A., & Chellappan, A. (2007). *Experimental studies on composite deck slabs to determine the shear-bond characteristic (m – k) values of the embossed profiled sheet. 63*, 791–803. https://doi.org/10.1016/j.jcsr.2006.07.009

Mohammed, B. S., Al-Ganad, M. A., & Abdullahi, M. (2011). Analytical and experimental studies on composite slabs utilising palm oil clinker concrete. *Construction and Building Materials, 25*(8), 3550–3560. https://doi.org/10.1016/j.conbuildmat.2011.03.048

Mohan Ganesh, G., Upadhyay, A., & Kaushik, S. K. (2005). Simplified design of composite slabs using slip block test. *Journal of Advanced Concrete Technology, 3*(3), 403–412. https://doi.org/10.3151/jact.3.403

Oehlers, D. J., & Bradford, M. A. (1995). 16 - Composite Profiled Slabs and Profiled Decking. In D. J. Oehlers & M. A. Bradford (Eds.), *Composite Steel and Concrete Structural Members* (pp. 381–406). Pergamon. https://doi.org/10.1016/B978-0-08-041919-0.50022-3

Raebel, C. H., Schultz, J. A., & Whitsell, B. (2020). Experimental investigation into acceptable design methods for cold-formed metal deck. *Journal of Constructional Steel Research, 172*, 106176. https://doi.org/10.1016/J.JCSR.2020.106176

Rahimi Mansour, F., Abu Bakar, S., Ibrahim, I. S., Marsono, A. K., & Marabi, B. (2015). Flexural performance of a precast concrete slab with steel fiber concrete topping. *Construction and Building Materials, 75*, 112–120. https://doi.org/10.1016/J.CONBUILDMAT.2014.09.112

Razaqpur, A. G., Lamberti, M., & Ascione, F. (2020). Debonding evolution in nonlinear FRP-retrofitted RC beams with cohesive interface. *Composite Structures, 236*, 111858. https://doi.org/10.1016/J.COMPSTRUCT.2020.111858

Saravanan, M., Marimuthu, V., Prabha, P., Arul Jayachandran, S., & Datta, D. (2012). Experimental investigations on composite slabs to evaluate longitudinal shear strength. *Steel and Composite Structures, 13*(5), 489–500. https://doi.org/10.12989/scs.2012.13.5.489

Smith, S. T., Hu, S., Kim, S. J., & Seracino, R. (2011). FRP-strengthened RC slabs anchored with FRP anchors. *Engineering Structures, 33*(4), 1075–1087. https://doi.org/10.1016/J.ENGSTRUCT.2010.11.018

Stark, J. (1978). DESIGN OF COMPOSITE FLOORS WITH PROFILED STEEL SHEET. *Proceedings - Annual Public Water Supply Engineers' Conference, 2*, 893–922.

Vainiūnas, P., Valivonis, J., Marčiukaitis, G., & Jonaitis, B. (2006). Analysis of longitudinal shear behaviour for composite steel and concrete slabs. *Journal of Constructional Steel Research, 62*(12), 1264–1269. https://doi.org/10.1016/j.jcsr.2006.04.019

Veljkovic, M. (1996). *Behaviour and resistance of composite slabs: experiments and finite element analysis.* Luleå tekniska universitet.

Wang, Y., Li, J., Deng, J., & Li, S. (2018). Bond behaviour of CFRP/steel strap joints exposed to overloading fatigue and wetting/drying cycles. *Engineering Structures, 172*, 1–12. https://doi.org/10.1016/J.ENGSTRUCT.2018.05.112

Widjaja, B. R. (1997). *Analysis and Design of Steel Deck – Concrete Composite Slabs Analysis and Design of Steel Deck – Concrete Composite Slabs*.

Wright, H. D., Evans, H. R., & Harding, P. W. (1987). The use of profiled steel sheeting in floor construction. *Journal of Constructional Steel Research, 7*(4), 279–295. https://doi.org/10.1016/0143-974X(87)90003-4

Zhang, D., Shi, H., Zhu, J., & Ueda, T. (2021). Analytical model for concrete cover separation of FRP strengthened RC beams with multiple steel bolts. *Structural Concrete, 22*(1), 183–197.

Zhou, C., Wang, L., Wang, Y., & Fang, Z. (2023). Experimental study on the flexural strengthening of one-way RC slabs with end-buckled and/or externally bonded CFRP sheets. *Engineering Structures, 282*(22), 115832. https://doi.org/10.1016/j.engstruct.2023.115832